The Marginal Ice Zone (MIZ) seawater property dynamics of the Southern Ocean below Southern Africa using animal-borne observations

WADE DE KOCK

DKCWAD001

Supervisor:

Assoc. Prof Marcello Vichi

February 2018

University of Cape Town

Department of Oceanography

MSc Mini Dissertation

National Research Foundation

PLAGIARISM DECLARATION

I know that plagiarism is wrong. Plagiarism is using another's work and to pretend that it is one's own.

I have used UCT Harvard as the convention for citation and referencing. Each significant contribution to, and quotation in, this proposal from the work, or works of other people has been attributed and has cited and referenced.

This thesis is my own work.

I have not allowed, and will not allow, anyone to copy my work with the intention of passing it off as his or her own work.

I acknowledge that copying someone else's work or parts of it is wrong, and declare that this is my own work.

SIGNATURE: Signed by candidate

DATE: March 2018

ACKNOWLEDGEMENTS

- I would like to thank my supervisor, Associate Professor Marcello Vichi for all the scientific help, knowledge and support.

- I am grateful to Dr Anne Treasure for providing the necessary processed data.

- My fellow classmates for all the coding assistance.

- This work is based on the research supported by the National Research Foundation, through the SANAP grant SNA14072880912.

- Mrs Nuroo Davids for the structural help and layout of my project.

- I am grateful to mother, Hildegard, and two brothers, Leigh and Gary, for their love and support.

ABSTRACT

The Marginal Ice Zone (MIZ) in the Southern Ocean is a dynamic area shown to vary seasonally in width and extent northward. Remote sensing is the only tool available to give a large-scale picture of sea-ice conditions but it is important to note that only surface properties are visible in remote sensing products. Little is known about the hydrographical properties of the Atlantic Sector of the Southern Ocean in the austral winter as it is difficult to obtain shipboard observations. Using observations from southern elephant seals, it is possible to analyse properties such as salinity and temperature within the MIZ. These properties may then be related to observations of sea ice concentration obtained by remote sensing to qualitatively describe their relationships. This work provides an example of how data from selected seal observations and satellite data can be used operationally to define the hydrography of the MIZ, focusing on the years 2005 to 2009. Results show that the properties of the underlying water in the MIZ appear to be fairly constant in the region of 15°W to 45°E for the months of July and August. A warmer pool of water is evident in the east of this region. Based on what is known about the physics of the region and what is seen spatially regarding changes in temperature and salinity, the warm pool may be brought about by eddies along the South West Indian Ridge. Results also show that surface concentrations of sea ice may have an effect on the underlying properties of the water. A more detailed description of the characteristics and features in the MIZ may further help to understand key processes in the region. Changes in subsurface temperature and salinity may influence the formation of ice. This may in turn influence large to mesoscale processes in both the ocean and atmosphere. Understanding how these physical properties change and what may cause them to change can help further understanding of larger scale processes.

Table of Contents

LIST OF FIGURES

1. INTRODUCTION

The Southern Ocean is dynamic and provides a major link between the three other ocean basins (Caldeira, 2000; Jacobs, 2006). The Southern Ocean also forms an integral part of global thermohaline circulation and is an area of convergence of several water masses (Sloyan et al., 2001; Gille, 2002). Its waters and the atmosphere above contribute importantly to global ocean circulation patterns and to the generation of storms (Andreas et al., 1984; Gille, 2002).

The Southern Ocean plays a pivotal role in the meridional overturning circulation (MOC) and is important for primary productivity and carbon dioxide draw down (Sloyan et al., 2001; Gille, 2002). It is therefore important for studies of the global carbon budget and global warming. The Southern Ocean is also home to a large number of organisms (Boyd et al., 2001). The biodiversity in the area confirms that the region also has considerable ecological importance (Boyd et al., 2001; Biuw et al., 2007).

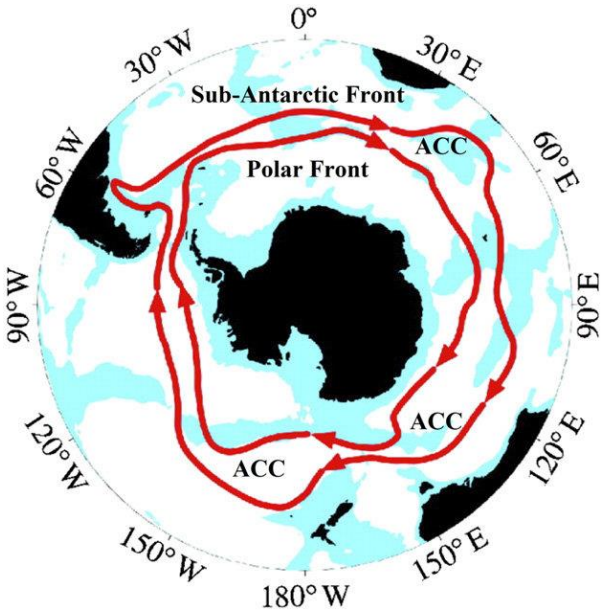

Figure 1: Map showing the Southern Ocean fronts. Map is as depicted by Constantin and Johnson (2016).

Complex frontal structures and ocean currents are found in the Southern Ocean contributing to primary productivity and adding to its highly productive nature (Fig. 1). The Sub-Antarctic Front (SAF) and the Polar Front (PF) show distinct temperature changes between two bodies of water (Belkin et al., 1996). The Antarctic Circumpolar Current (ACC), which is the world's largest ocean current, lies between these two fronts. The ACC also reacts with the continental shelf of Antarctica to form the Weddell gyre which also influences the Southern Ocean's frontal structure (Park et al., 2001). Belkin et al. (1996) suggest that the region south of Africa introduces the Agulhas Retroflection (AR) into the SAF. The AR influences the SAF and this in turn affects the other surrounding frontal systems and the ACC. This convoluted interaction between frontal systems has effects on surrounding physical and atmospheric characteristics.

Another factor that influences the physical characteristics of the Southern Ocean and its ecology is the presence of sea ice (Belkin et al., 1996; Drucker et al., 2003). Sea ice or the lack thereof contributes to the formation of water masses in the Southern Ocean (Park et al., 1998). It is important to observe and understand the spatial and temporal variability of sea ice in this regard. The area seasonally influenced by sea ice is known as the Marginal Ice Zone.

1.1. Observations of the Marginal Ice Zone (MIZ) in the Southern Ocean

1.1.1. The MIZ and its impact on the surrounding ocean

The area of transition from open ocean to consolidated sea ice is known as the Marginal Ice Zone (MIZ) (Wadhams et al., 1988). This is a dynamic region influenced by the physical features of the ocean and atmosphere (Wadhams et al., 1988). The extent of sea ice within the MIZ is based on the formation and melting of sea ice. The formation of sea ice plays an important role in changes of the physical properties of the surrounding waters because it changes the temperature and increases the salinity of the remaining water (Weeks and Ackley, 1986; Fletcher, 2009). Sea ice thus has a large influence on the physical and also biogeochemical properties of the surrounding waters, so understanding changes of sea ice both spatially and temporally may help understand processes in more detail (Fletcher, 2009; Aoki et al., 2013; Ohshima et al., 2013). Aoki et al. (2013) found that there is a freshening in the MIZ at 140°E off Antarctica. Occurrences such as those found by Aoki et al. (2013) may

provide some insight as to how physical features such as salinity and temperature change in certain areas. Ohshima et al. (2013) also report on how the formation of Antarctic Bottom Water is tied to the formation of sea ice. This shows how linked the seasonal sea ice is to the physical properties of the water, which is particularly important in an era of climate change when processes change in pronounced ways.

Antarctic sea ice is dynamic in the way it shifts. Sea ice is formed in diverse ways and the ice floes themselves may be different in size and structure (Bjorgo et al., 1997). Ice formation occurs with cooling water temperatures (Weeks et al., 1986). Fresher water starts to freeze, and brine rejection occurs causing an increase in salinity (Weeks and Ackley, 1986). These processes are particularly important in the upper layer of the ocean (Weeks and Ackley, 1986). The Mixed Layer Depth (MLD) of the ocean may change based on wind mixing and other physical processes. These effects become less apparent closer to consolidated sea ice (Martinson, 1990). There is less of an immediate heat exchange between the ocean and atmosphere (Weeks and Ackley, 1986). This influences the way water masses behave: mixing and turbulence brought on by the atmosphere decrease (Weeks and Ackley, 1986). The formation of sea ice has direct impacts on the underlying water (Aoki et al., 2013). This is also demonstrated by Ohshima et al. (2013) who closely link the density of water to areas of seasonal sea ice. The larger the area of sea ice cover, the more of an effect it will have on the underlying waters (Martinson, 1990).

1.2. Factors influencing sea-ice formation

1.2.1. Thermohaline circulation

External forces other than atmospheric forcing may influence the formation and melting of ice in the region (Fletcher, 2007). Behrendt et al. (2011) illustrates how sea ice may influence water mass formation and movement. Ohshima et al. (2013) also suggests that water mass formation in the form of Antarctic Bottom Water may also influence the sea ice. From these two studies, it is evident that the slow formation of water masses plays a role in the presence of sea ice. In addition to the formation of Antarctic Bottom Water in the formation, Behrendt et al. (2007) indicate that there are warm deeper waters (WDW) and colder winter water (WW) surface layer in the Atlantic sector of the Southern Ocean. WW may promote the

formation of sea ice in the MIZ. Changes in WW and WDW may be related to Southern Ocean fronts. In order to improve understanding on the formation of sea ice it is important to understand the water masses in the region (Orsi et al. 1995).

Temperature-Salinity (TS) diagrams are used to characterize water masses. They indicate the effects of sea ice in the MIZ which becomes important in the austral winter.

a)

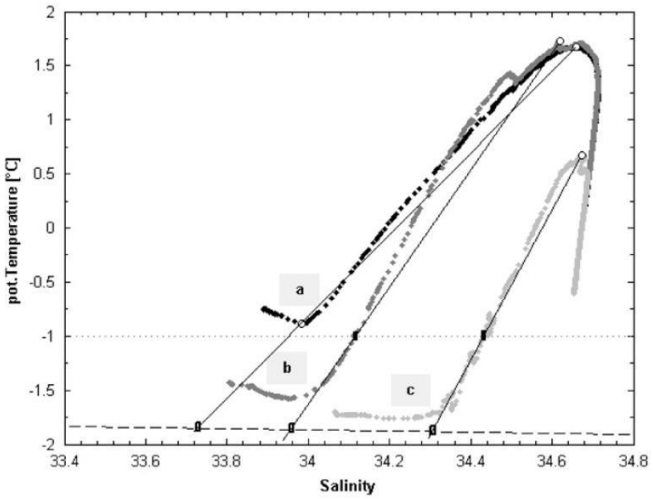

b)

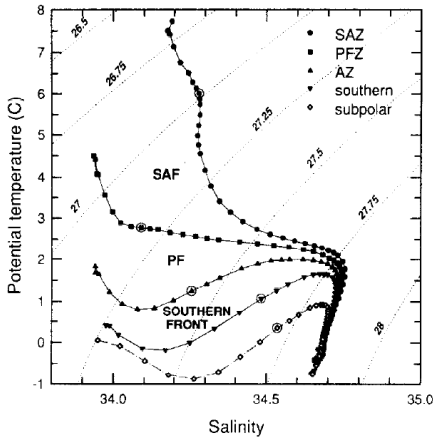

Figure 2: Reference TS (Temperature-Salinity) diagrams taken from Behrendt et al., 2011(a) and Orsi et al., 1995 (b). These water analyses show typical water masses around Antarctica. Temperature is measured in degrees Celsius and salinity in practical salinity units (psu).

Typical patterns in temperature and salinity are shown (Fig. 2) for the MIZ of the Southern Ocean. TS diagrams from Orsi et al. (1995) show that frontal differences in the Southern Ocean are strong, with temperatures ranging from -2 to 2 °C (Fig. 2b). The presence of sharp differences in temperature limits the regions of formation of sea ice. Salinity also ranges from 33.8 to 34.7 psu (practical salinity units). In the MIZ both temperatures and salinities increase

with depth until they reach a density where temperatures drop and salinities remain fairly consistent. Changes in temperature and salinity are frontal related: south of the PF, temperatures initially decrease with depth and then increase as salinities increase with depth to roughly 34.7 psu.

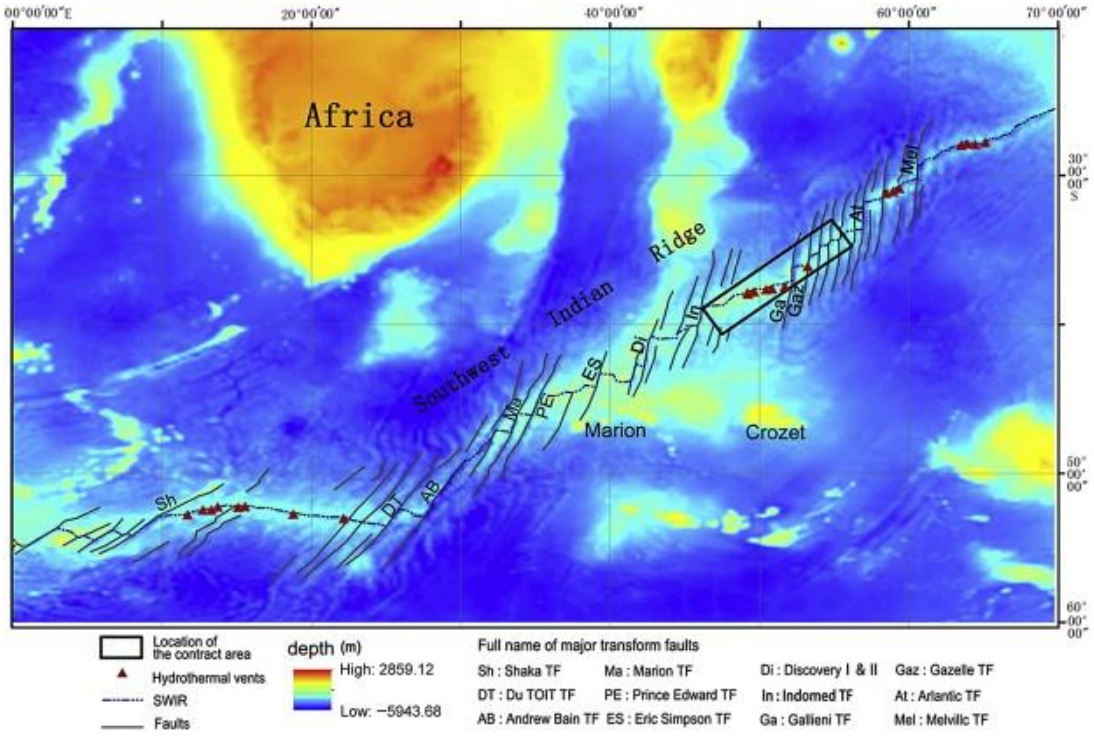

Figure 3: Map showing the South West Indian Ocean Ridge(SWIR) along with the Southern Ocean islands Marion and Crozet. Map is as depicted by Ren et al. (2015).

1.2.2. The role of mesoscale eddies

The movement of water influences the formation of sea ice (Martinson 1990). The South West Indian Ocean Ridge (Fig. 3) causes prominent eddy activity (Shimada et al., 2006). The generation of these eddies may include changes in the physical properties of the water (Foster et al., 1976). If these eddies are transported southwards, they may influence the formation and distribution of ice (Shimada et al., 2006). The transport of these eddies also causes changes in the biogeochemistry and productivity of the region (Carmack, 2007). Massie et al. (2016) demonstrate how the eddy field generated by the South West Indian Ocean Ridge (SWIR) has an effect on productivity and they show how these changes in productivity influence southern elephant seal foraging techniques, location and behaviour. Durgadoo et al. (2010) also report

that the advection of these eddies creates temporary areas which are seen as biologically productive. Ansorge et al. (2010) have shown that these eddies may have cores of 2.5 °C down to 200 m depth, with fresher surface salinities rising to above 34 psu with depth. Their link with sea ice dynamics is however speculative, as it remains difficult to monitor features like eddies and to track them in winter.

1.2.3. Air-sea interaction

In the winter months, storms in the region promote mixing (Mitchell et al, 1991; Park et al., 1998). An increase in mixing causes a deeper MLD as waters are now more turbulent (Park et al., 1998). At the same time as this, ice forms with the maximum ice extent occurring in October at the end of winter (Gloersen and Campbell, 1991). Ice formation increases stratification as salinity increases results in a shallower MLD (Weeks and Ackley, 1986; Park et al., 1998). Temperature and salinity then become more uniform closer towards consolidated ice and the Antarctic shelf (Adkins et al., 2002). This is also a time when ship-based observations are rare (Worby et al., 2008; Weissling et al., 2009).

1.3. Observing the Southern Ocean

Despite the Southern Ocean's major contribution to earth systems, it is still relatively under-sampled compared to the world's oceans (Gould et al., 2004; Boehme et al., 2009; Charrassin et al., 2010; Fedak et al., 2013; Roquet et al., 2014; Riser et al., 2016). Ship-based sampling in the Southern Ocean is usually associated with supplying Antarctic bases in summer and is rare in winter months (Fedak, 2013; Roquet et al., 2013). Models rely heavily on observations in order to resolve unique features of the Southern Ocean (Steele, 2004). There is also a need for *in situ* data to validate satellite observations such as the extent of sea ice (Worby et al., 2008).

The remoteness of the region means that scientists have to rely on alternative methods of *in situ* observation (Reynolds et al., 2002; Biuw et al., 2007; Biuw et al., 2010; Riser et al., 2016). ARGO floats, ice floats, gliders, buoys and ice trackers are ways of obtaining in situ data in and around the Southern Ocean without having to be on a ship (Gould et al., 2004; Freeland et al., 2010; Riser et al., 2016). Many of these instruments require the aid of ships

for their deployment, but they may be monitored using satellite technology (Roemmich et al., 2004). The remote observations also continue for longer periods of time compared to ship-based measurements, depending on battery life and sampling frequency (Gould et al., 2004; Riser et al., 2016). Effective sampling with depth requires the instrument to resurface (Boehme et al., 2008) for instruments to transmit data to satellites by radio. This is a challenge in the Southern Ocean where sea ice cover changes over time, and is particularly so in winter when sea ice cover increases substantially (Kikuchi et al., 2007).

1.4. Observing sea ice

Further research is needed to better understand the processes occurring in the region of variable sea ice (Kikuchi et al., 2007), particularly in the austral winter. Many methods of sampling are used in the Southern Ocean. This present study will focus on two methods of sampling.

1.4.1. Satellite imagery

Observations in and around sea ice are currently difficult to obtain. There are visual and practical ways of measuring sea ice in the Antarctic such as the Antarctic Sea ice Processes and Climate method (ASPeCt) (Worby et al., 2008; Weissling et al., 2009). These observations are either ship-based or airborne (Worby et al., 2008). Though useful, it is impractical to continually observe the ice all year round in this manner (Brierley et al., 2002). Scientists therefore rely heavily on satellite imagery (Zhang and Skjetne, 2015). Special Sensor Microwave Imager (SSMI), Special Sensor Microwave Imager Sounder (SSMI/S) and the Advanced Microwave Scanning Radiometer - Earth Observing System (AMSR-E) are passive satellite radiometers on near polar orbiting satellites (Turk and Miller, 2005). Passive microwave sensors like those mentioned above require sunlight to work (Gloersen et al., 1993). This may be problematic for long periods of time during winter. This is particularly challenging when trying to define the start of the ice edge (Strong et al., 2017).A target or area is illuminated with and an antenna detects photons at particular microwave frequencies. The signals are then reflected to show differences in the ocean surface (Comiso et al., 2008; Strong et al., 2017). The pulse reflected back from sea ice is different to that of its

surrounding waters (Gloersen et al., 1993). Some ice types are difficult to detect using backscatter (Strong et al., 2017).

The MIZ shows a range of ice types and structures (Clarke and Ackley, 1984). Grease ice for example, shows no apparent change to the colour of the surrounding waters. This is particularly an issue at higher latitudes where the MIZ starts (Drucker et al., 2003). This area shows a large presence of grease ice (Clarke and Ackley, 1984). It is therefore difficult to show where ice formation starts to occur (Espedal et al., 1996; Drucker et al., 2003). Spatial resolution of satellite products has improved over the years due to improved technology (Drucker et al., 2003).

Sea Ice Concentration (SIC) is one of the measurements derived from passive sensors (Comiso et al., 1997; Hall et al., 2002). This is done using specific algorithms to predict sea ice from backscatter (Comiso et al., 1997; Hall and Visbeck, 2002). Satellite observations of sea ice have proven useful over the last four decades and are continually improving in terms of resolution, prediction and coverage (Comiso et al., 2008). Processes that occur due to the formation and melting of sea ice have proven to be both relevant and useful when explaining the effects sea ice may have on the surrounding waters (Toudal, 1999; Toyota et al., 1999; Russell et al., 2006).

1.4.2. CTD-SRDL Observations

Autonomous observations as well as remote observations are needed in the Southern Ocean during the winter months (Boehme et al., 2009). Few floats or marine instruments can measure in areas of high sea ice cover (Roquet et al., 2013; Riser et al., 2016). A recent method used for measuring hydrographic properties in the MIZ is tagging marine mammals with sensors (Biuw et al., 2007; Boehme et al., 2009). Marine Mammals Exploring Oceans from Pole to Pole (MEOP), http://www.meop.net/, is a programme for using marine mammals as vehicles to collect valuable data. The programme is also responsible for tagging the animals.

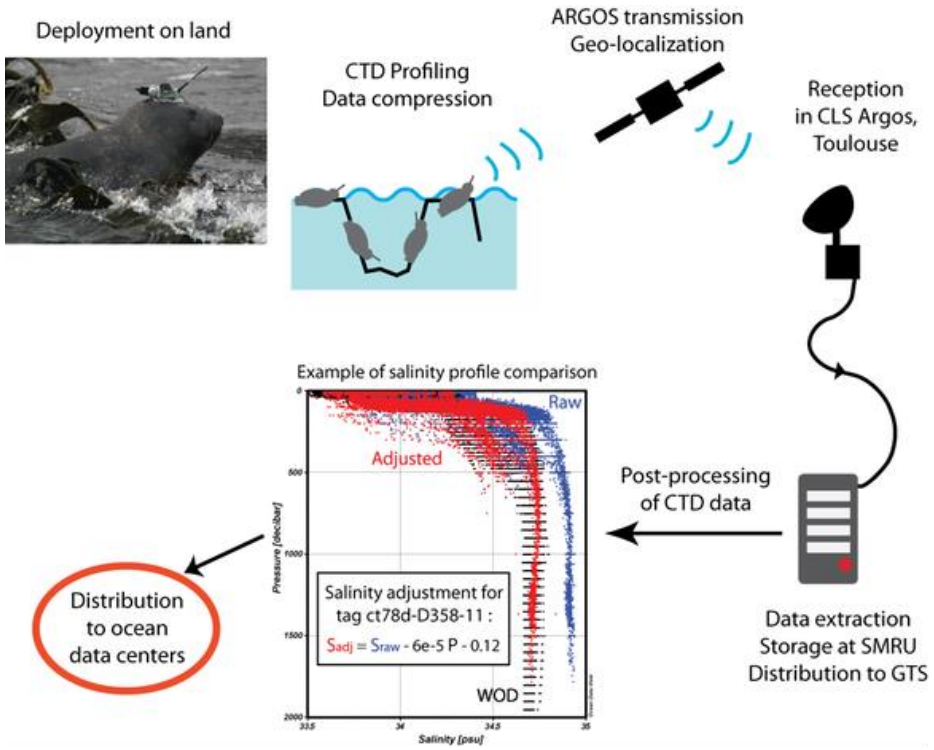

Figure 4: Tagging and processing of the CTD-SRDL tags. Sourced from the MEOP database (http://www.meop.net/meop-portal/about-meop.html)

Conductivity Temperature Depth- Satellite Relay Data Loggers (CTD-SRDLs) are used on marine mammals to monitor their behaviour and habitat conditions. Following the initial objective, these instruments also provide useful hydrographic information (Fedak, 2004; Roquet et al., 2014). In the Southern Ocean, southern elephant seals (*Mirounga leonina*) are typically tagged with these devices (Fig. 3). The elephant seals are tagged on the top of their heads in such a way that it does not hinder the animal's well-being, manoeuvrability and its means for survival (Fedak, 2004).

Southern elephant seals spend long periods of time foraging and the hydrographic information is collected on the seal's ascent to the surface (Biuw et al., 2007). The data is then collected by the ARGOS satellite system (Roquet et al., 2013). The data is then processed at the Sea Mammal Research Unit – Instrumentation Group (SMRU-IG) in Scotland (Roquet et al., 2013). This provides scientists with physical properties of the waters surrounding the animals which were previously unavailable at such a high resolution (Roquet et al., 2013; Massie et al., 2016). This is particularly useful in ice-covered areas where instruments such as ARGO floats may have a resurfacing issue (Kikuchi et al., 2007).

The CTD-SRDL tags fall off during the animal's annual moult which takes place between late spring and early summer (Biuw et al., 2007). Late spring and summer coincides with the breeding behaviour of the elephant seal so, in many cases, these tags may be collected on islands where the seals breed (Fig. 2) (Boehme et al., 2008; Fedak, 2004). This tagging method has proven useful in several studies (Boehme et al., 2008; Charrassin et al., 2008; Massie et al., 2016).

However, the ecology of the southern elephant seal needs to be considered (McIntyre et al., 2011). The seals have a tendency to travel and forage in particular areas (Biuw et al., 2007). This may coincide with where food sources, mainly cephalopods such as squid and octopus, are abundant or where pack ice does not occur (Biuw et al., 2007). The diving behaviour of the southern elephant seal may vary seasonally as well as diurnally (Biuw et al., 2007). Seal foraging behaviour has shown to shift from a pelagic to a benthic region (Meredith and Hogg, 2006; Massie et al., 2016). This may affect how the seals dive and the hydrographic information collected on these dives.

The southern elephant seals spend a considerable amount of time foraging further south in the austral winter (Biuw et al., 2007; Charrassin et al., 2008). This may depend on their ecological behaviour or the availability of food (Boehme et al., 2008; Carrick et al., 1962). This would mean that the number of dives spent in and around the MIZ increases in the austral winter months (Boehme et al., 2008; McIntyre et al., 2011). Consequently, CTD-SRDL observations would increase in the austral months when observations from ship-based methods are few (Biuw et al., 2007; Boehme et al., 2008; Fedak 2013). The region of the MIZ is also seen as biologically productive (Massie et al., 2016). Using CTD-SRDL observations comes at an advantage in the MIZ. The more time seals spend diving the more samples are collected and partial sea ice cover does not seem to hinder the movements or foraging capabilities of the seals.

The Sub-Antarctic (SAF) front and Polar Front (PF) are regions that show a high concentration of seal dives (Fig. 1) (Boehme et al., 2008). High primary productivity occurs along these fronts and this may be translated to the availability of food for the southern elephant seals (Charrassin et al., 2008). Temporally, foraging as result number of recorded dives, show to be at a maximum during the months of late autumn to early spring (Charrassin et al., 2008). Southern elephant seals have to return to land in order to breed and rear pups

(Carrick et al., 1962);this confines them to land for the period of late spring to summer thus decreasing the number of dives in remote regions of the Southern Ocean (Carrick et al., 1962).

The hydrographic information depends strongly on the foraging behaviour of these seals as well as their breeding grounds (Biuw et al., 2007). Previous studies have shown that southern elephant seals spend copious amounts of time around the Antarctic shelf as well as the Southern Ocean fronts (Massie et al., 2016). These foraging areas may differ seasonally based on their life history as well as the availability of food (Biuw et al., 2007; Biuw et al., 2010).

CTD-SRDL observations have proven useful in previous studies e.g. (Biuw et al., 2007; Boehme et al. 2009; Fedak et al., 2013; Ohshima et al., 2013; Roquet et al., 2014; Massie et al., 2016) but have not been analysed specifically in the MIZ. Ohshima et al. (2013) does however use instrumented seal data to analyse Antarctic Bottom Water formation, linking areas of ice formation to the formation of Antarctic Bottom Water. In doing so, the paper shows new ways of using CTD-SRDL data and suggests the influence of ice formation on the surrounding waters. Since the extent of the MIZ may vary seasonally as well as annually, the physical features would change with latitude over time. This change in physical properties may then be used when monitoring the MIZ and in Southern Ocean models.

1.5. Objectives

The aim of this study is to qualitatively relate Sea Ice Concentration (SIC) in the MIZ to the hydrographic details provided by CTD-SRDL tags attached to elephant seals. Sea ice data from satellites are used to give an estimate of SIC over winter and the relationship between sea ice and the physical properties is examined.

The concurrent analysis of sea ice and seawater properties may help to relate sea ice distribution and features in the MIZ to the underlying seawater properties. This would indicate whether the underlying seawater and its changes potentially influence the extent of the MIZ or not.

2. METHODOLOGY

In order to visualise the spatial and temporal distribution of the CTD-SRDL data, two satellite products of SIC were considered for the years 2005 to 2009. The consistency and validity of the SIC satellite observations were then analysed using in situ CTD-SRDL observations.

2.1. Defining the MIZ using remote sensing data

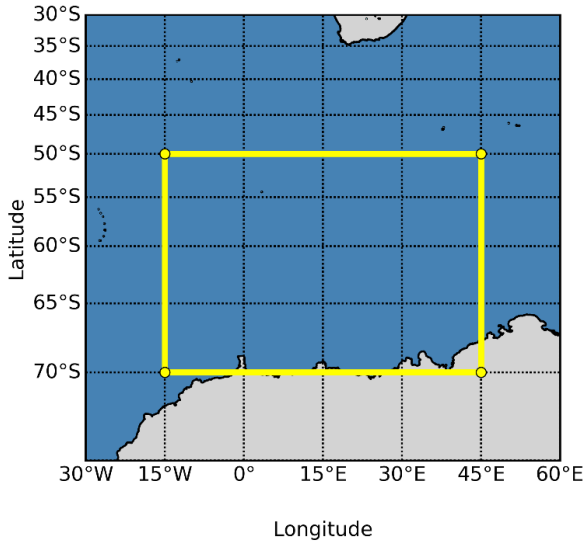

Figure 5: Area of study south of South Africa

The study region was selected as 15°W to 45°E and 50°S to 70°S (Fig. 5), which encapsulates the MIZ south of Southern Africa. The SIC maps are derived from the satellite sensors SSMI/S on satellite DMSP-16 and AMSR-E on satellite AQUA. Both products are available between 1 January 2005 and 31 December 2009, the period of study. The ASI (Arctic Sea Ice) algorithm (Kaleschke et al., 2001; Spreen et al., 2008) was used with both products to calculate sea ice concentration. The data was obtained from the Integrated Climate Date Centre (ICDC, ftp://ftp-icdc.cen.uni-hamburg.de/), University of Hamburg, Hamburg, Germany. The data obtained from each satellite have 25 km resolution and are daily data in netCDF (Network Common Data Form) format. The daily data had to be pre-

processed to monthly datasets. Once monthly averages were calculated, the monthly climatology was computed for both the AMSR-E and SSMI/S sea ice products.

Since one aim of the work is to identify the hydrographical conditions corresponding to the MIZ and whether the satellite data can provide this location adequately, the use of the 15% threshold (Stroeve and Campbell, 2016) needs to be properly implemented. The geographical location of the 15% SIC line for each satellite product was obtained by identifying pixels which ranged in the concentrations between 13-17% SIC. This was done by creating a subset of concentrations for this range. The subset was then plotted on a bar graph. The distribution of these pixels indicates which measure of central tendency should be used when working out an estimated latitude value of sea ice extent for each period of the year at a given longitude. Box and whisker plots were made to indicate which measure of central tendency should be used. An average may be heavily biased by the multi-modality as was seen in the bar graphs. A more robust indicator for the spread of the data was thus needed and it was decided to use the median as the measure of central tendency.

Since the approximation of medians was similar in the months of July and August concerning both sensors, an analysis needed to be done to see whether or not the same is true for the rest of the months of the year. A time series for both satellite sensors was plotted for the monthly medians of the 15% and 80% SIC lines. The area between these lines gives a working definition of the MIZ for the purposes of this study

Upon geographic visualisation, Python version 3.6.0 was used to map monthly sea ice concentrations in the study region for each month of the year (Appendix A). The focus of this study is on July and August due to the increase of sea ice in these months.

A five-year average of SIC and five years of CTD-SRDL observations were used for the region. This was done by analysing the average MIZ distribution for the years 2005 to 2009. These years coincide with an increase in CTD-SRDL observations. Each month of the year was compared visually using the Python mapping tool . The average 15% and 80% contour lines were plotted for each month. The visual space between these lines was considered to be the operational extent of the MIZ for this study.

2.2. Mapping CTD-SRDL observations in the MIZ

The CTD-SRDL data were obtained from the MEOP database (http://www.meop.net/database/) in .csv format. The data includes tagging and gender details. Information obtained from the southern elephant seals is transmitted only when the seals dive and resurface (Roquet et al., 2013). Fifteen stations then receive the data which is then processed at the Sea Mammal Research Unit Instrumentation Group (SMRU-IG), Scotland (Fedak, 2013). The Doppler Shift Effect is used to determine the location of the CTD-SRDL data (Fedak, 2013). Recent years have shown an increase in spatial resolution of this data. Physical property measurements of the water such as salinity and temperature have also improved with respect to accuracy and precision (Fedak, 2013; Massie et al., 2016).

The CTD-observations were from the study period 2005-2009. Twelve monthly subsets were created for the CTD-SRDL observations over the five years. For this study the subsets of July and August were considered. The two subsets were also filtered based on longitude and latitude range. The same longitude and latitude range used when defining the MIZ was considered (Fig. 5). Each southern elephant seal has a unique seal ID. Each seal also dives multiple times, and these dives are monitored by having unique station numbers. Specific seals or specific dives from the subsets may then be obtained by using the necessary criteria to filter. It is also important to note that the seals were all tagged in the time span of 2005 to 2009 so any inter-annual variability would need to be taken into consideration if seals from different years are compared.

Southern elephant seal dives were counted between the estimated 15% and 80% SIC lines. A count was done for both the SSMI/S and AMSR-E satellite sensors. The CTD-SRDL observations within the MIZ were then plotted on the maps of the MIZ extent. The maps indicated how many seals dived within the MIZ. The CTD-SRDL observations beyond the MIZ and closer to open waters were then also plotted to visually indicate how often seals dived in the MIZ. A monthly bar graph was then plotted to count the number of seal dives in the MIZ over the 5 years. This further confirmed the use of the months of July and August as these two months showed more than 85% of seal dives in the MIZ.

2.3. Plotting subsurface physical properties using CTD-SRDL observations

CTD-SRDL observations were selected based on their seal IDs as well as their locations within the MIZ and outside of it.

Sets of CTD-SRDL observations were selected from the data for the months of July and August. The area of interest for this study was the MIZ. H

For each month, two seals were selected for the open ocean where there was little to no sea ice. Three seals were selected around and within the MIZ and one seal was selected south of the MIZ where sea ice concentrations are higher than 80%. Temperature and salinity sections were then plotted for each southern elephant seal to note any general differences or similarities among the three regions.

After noting differences in temperature and salinity among the three regions, it was important to see how these changes propagate with latitude within the MIZ. Specific profiles of temperature and salinity for each seal were then plotted to see how physical properties may change with respect to changes in latitude.

Seal dive trajectories which overlap were also compared to one another as well as seals that foraged parallel to the MIZ. This was done to account for any changes or similarities. Trajectories parallel to the MIZ may account for physical differences with longitude. Sea ice cover may change zonally so comparing parallel trajectories may explain any apparent effects a changing concentration of sea ice.

Cross sections of specific seal dives were performed using Ocean Data View (https://odv.awi.de, 2017). The interpolation was executed using the DIVA gridding algorithm (Troupin et al., 2012), which is a form of analysis of variance. The cross section also shows the original points for each seal dive in order to account for the distribution of the data. The SIC lines of 15% were added to the cross section for both the AMSR-E and SSMI/S satellite sensors which show changes with latitude. This may display the effect of sea ice on salinity and temperature. It may also indicate which satellite estimate corresponds best with the hydrographic changes. Along with the cross sections of each track, changes in SIC are plotted. Sea ice concentrations were considered using daily data at the time each dive took

place. The SIC was then recorded for the position of each profile. Finally, temperature-Salinity (TS) diagrams were plotted in order to identify water masses in the study region.

3. RESULTS

3.1 Seal dives within the MIZ boundaries

a)

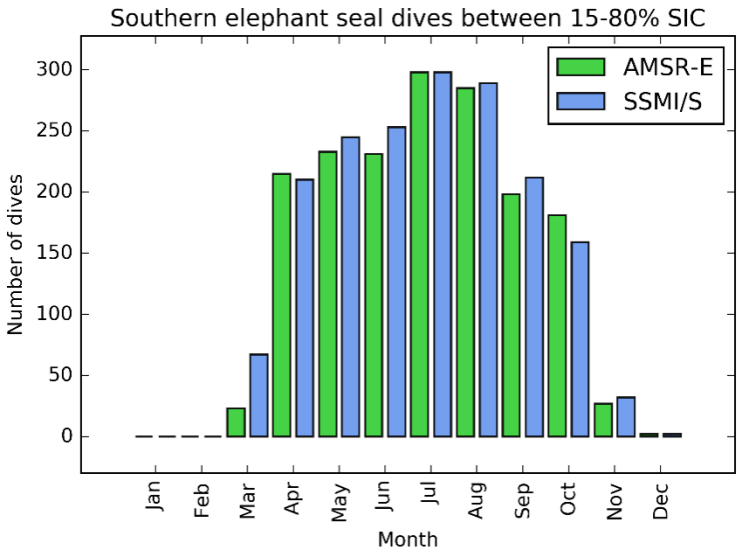

b)

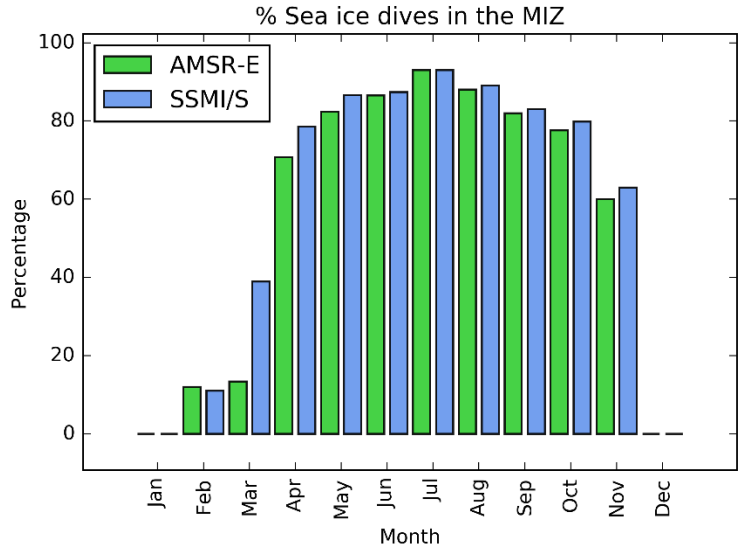

Figure 6: Number of southern elephant seal dives between 15%-80% SIC determined using satellite sensors AMSR-E (green) and SSMI/S (blue) for the years 2005-2009. (a) shows the number of dives counted within the MIZ. (b) shows the percentage of dives in the MIZ out of all dives in the study region each month.

To verify usable CTD-SRDL observations, the locations of the data need to be related to the MIZ, using the area between 15% and 80% SIC as described in the methods section. The temporal distribution of CTD-SRDL observations is fairly consistent for both the AMSR-E and SSMI/S sensor readings (Fig. 6). The maximum number of observations occurs in the

austral winter months of July and August. Fewer dives occurred in the summer months. Autumn and spring months show varying numbers of observations of both sensors. These differences are caused by the difference in the location of the 15% and 80% SIC lines for the two products, especially in March.

The proportion of total dives in the MIZ is at its maximum during the austral winter (Fig. 6b), indicating that the seals spend the majority of their time in winter in this region. The most dives in the MIZ occur in June, July and August. The percentage of dives then decreases as the ice retreats and the breeding season for seals starts.

a)

b)

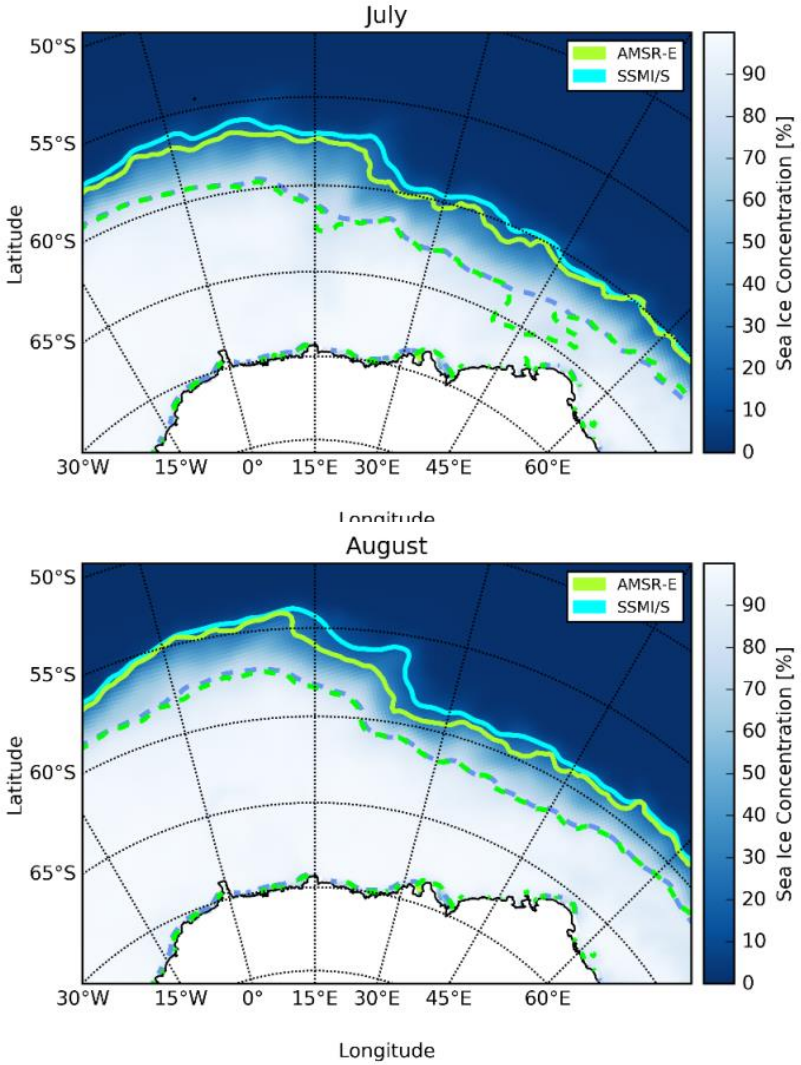

Figure 7: 2005-2009 Average sea ice concentration for July (a) and August (b) using the AMSR-E sensor (green) and SSMI/S sensor (blue). The solid lines represent the 15% SIC line and the dashed lines represent the 80% SIC line. The area between them is defined as the MIZ for this study. The additional 80% SIC lines at the Antarctic coast are artefacts of coastal contamination (Serreze et al., 2003) and are therefore ignored in this study.

Sea ice occurs furthest north in the west of the study region (Fig. 7). August shows an increase in SIC with the MIZ being wider in August than July. It is interesting to note the SSMI/S sensor shows approximations of the 15% SIC line to be slightly north of the AMSR-E line in both the months of July and August. The 80% SIC line is shown to be similar in both satellite sensor approximations. The western side of the MIZ is wider and progresses further northward than the eastern side.

3.2 Analysing the MIZ boundaries using remote sensing observations

a)

b)

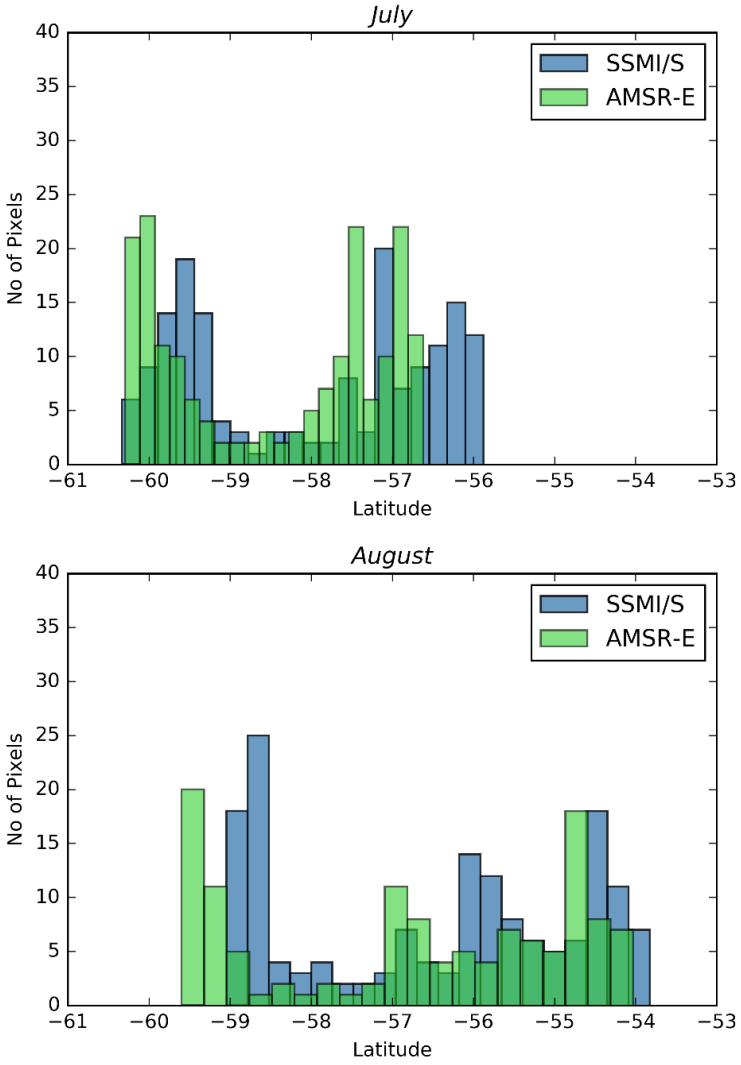

Figure 8: Counts showing the distribution of latitude of the 15% SIC line in the months of (a) July and (b) August using the AMSR-E (green) and SSMI/S (blue) satellite sensors. This was done for the period 2005-2009.

The distribution of latitude of the northern MIZ edge (15% SIC) for the region of 15°W to 45°E appears to be bimodal during July (Fig. 8a). This distribution applies to both the AMSR-E and SSMI/S sensors. SSMI/S however, shows that the MIZ extends further northwards compared to the MIZ extent of the satellite sensor AMSR-E. Consequently, more seal observations are seen to lie within the MIZ using the SSMI/S sensor (Fig. 6a). The AMSR-E sensor on the other hand shows more observations around 60°S as it extends further south. The month of August (Fig. 8b) appears have a multimodal (rather than bimodal) MIZ boundary in both datasets. With regards to the AMSR-E sensor, more observations appear to occur around 59.5°S, 57°S and 55°S. 57°S shows large numbers of observations by both satellite sensors in July. Based on the changes in the distribution of observations, sea ice does not advance evenly at all longitudes. This is also seen in the sea ice concentration maps for July and August (Fig. 7).

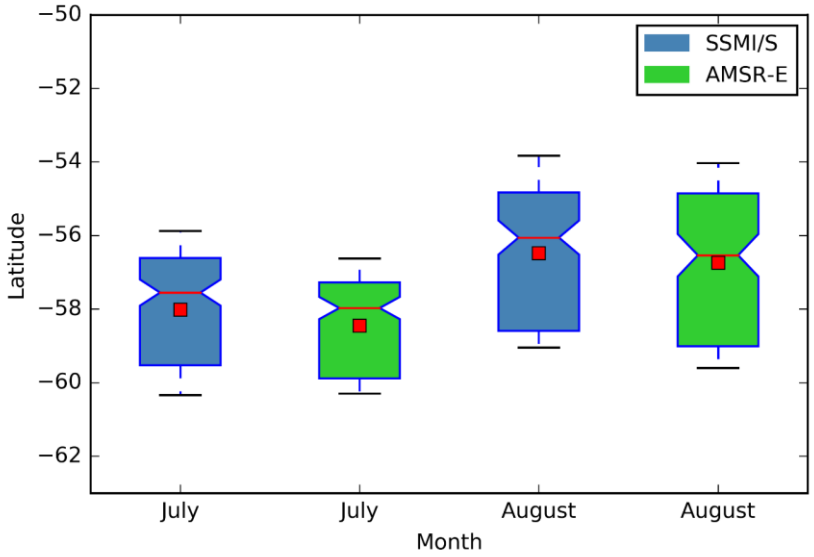

Figure 9: Box and whisker plot showing the latitudinal distribution of the 15% SIC (number of pixels) in the Atlantic sector using the satellite sensors AMSR-E (green) and SSMI/S (blue) for the months of July and August. The red square on each distribution plot represents the mean latitude of the 15% SIC. The red line represents the median (Q2) of each dataset. The top of each box represents the third quartile (Q3) and the lower end of each box represents the first quartile (Q1). After removing all outliers by identifying the maximum and minimum latitudes, the upper black lines represent the minimum latitude (northward) and the lower black lines represent the maximum latitude (furthest south).

The northward shift in the MIZ edge from July to August appears in both the AMSR-E and SSMI/S sensor observations (Fig. 9). The range of the latitude from maximum to minimum

also increases in both sensors for the month of August. Both the means and medians for SSMI/S are slightly more north for July and August. This northwards shift may be seen in the distribution plots (Fig. 8) as well as the sea ice concentrations maps for July and August (Fig. 7). Both satellite sensors show similar distributions and ranges (Fig. 9). Both satellite sensors show an increase of 2° north from July to August which indicates that the MIZ is further north in August (top black lines).

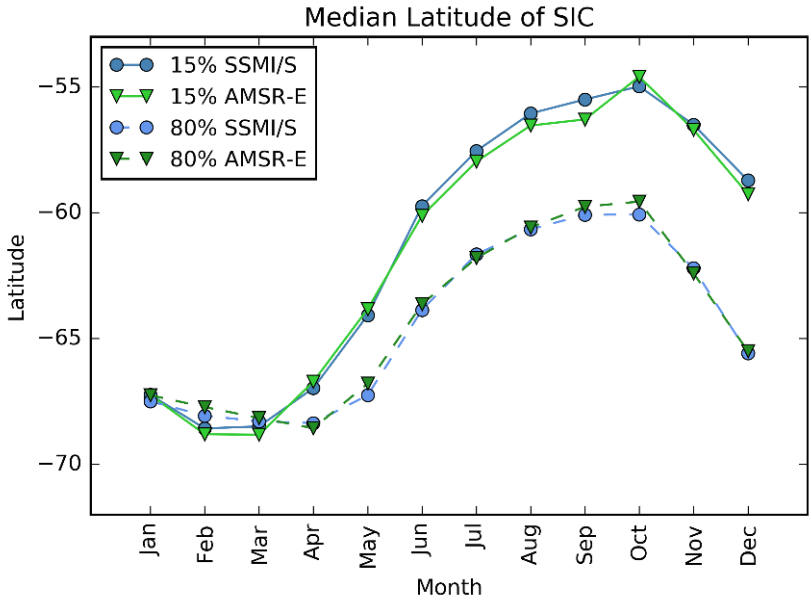

Figure 10: The 5-year average of 2005- 2009 for the monthly median latitude of the Marginal Ice Zone (MIZ). This is represented by the 15% SIC line (continuous lines) and 80% SIC line (broken lines) using the satellite sensors AMSR-E (green) and SSMI (blue).

Similar monthly distributions are seen in both sensors for the 15% and 80% SIC lines (Fig. 10). The 80% SIC latitude is almost identical for the AMSR-E and SSMI/S sensors. SSMI/S, however, still indicates a 15% SIC latitude slightly north than that of the AMSR-E sensor as seen in the box and whisker plot of latitudinal distribution for the winter months (Fig. 9). The months of January, February and March show little differences between the 15% and 80% SIC lines as there is little to no sea ice present during these months.

It is important to note the increase in latitudinal range of the MIZ towards the austral winter in the case of both satellite sensors. This northward extent increases until the month of October where the MIZ extent is greatest.

3.3 The relationship between CTD-SRDL observations and the MIZ

a)

b)

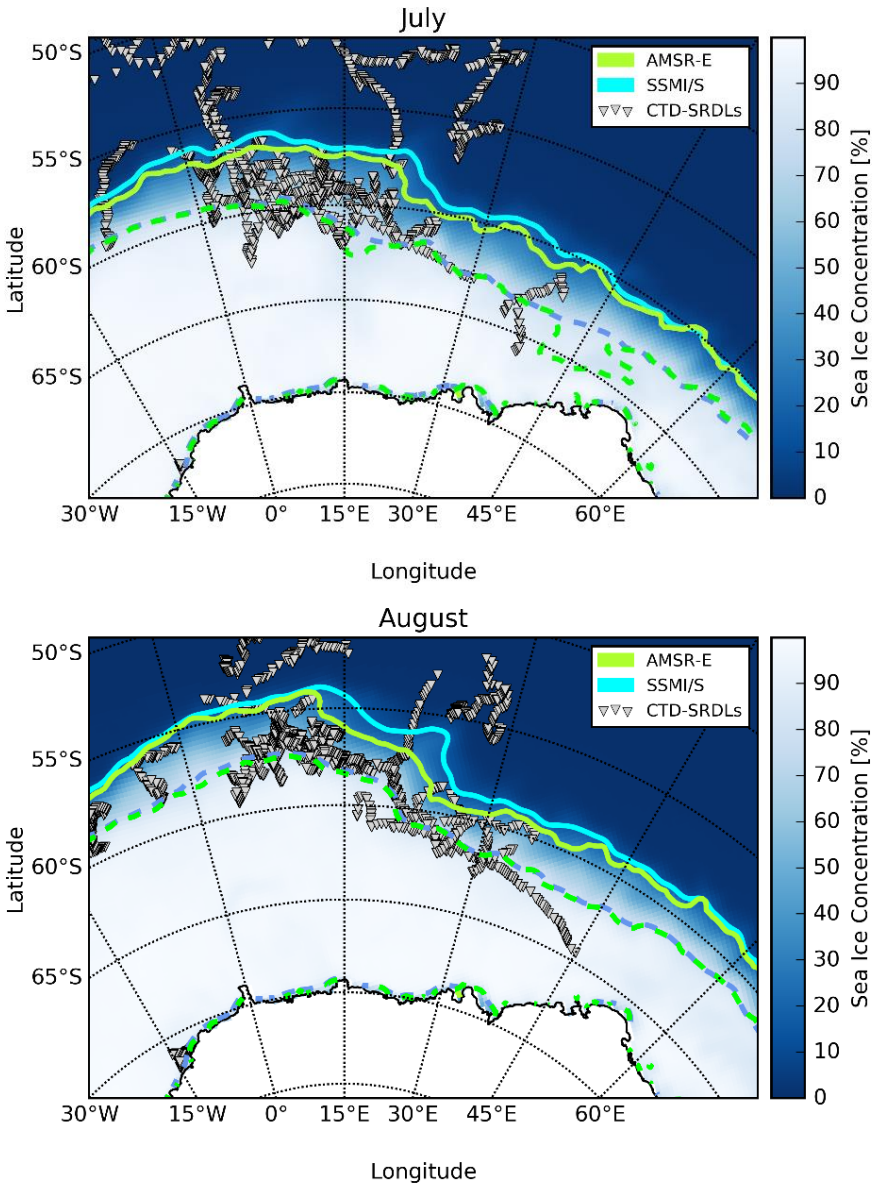

Figure 11: 2005-2009 Average sea ice concentration for July (a) and August (b) using the AMSR-E sensor (green) and SSMI/S sensor (blue). The solid lines represent the 15% SIC line and the dashed lines represent the 80% SIC line. The points on each map (grey) indicate the geographic distribution of seal diving observations from the MEOP database for the years 2005-2009. The additional 80% SIC lines at the Antarctic coast are due to coastal contamination (Serreze et al., 2003) and are thus ignored in this study.

There are many CTD-SRDL observations in the MIZ during both July (298) and August (287) (Fig. 11). During these months southern elephant seal dives extend further south than the 80% SIC line. The finding in Section 3.1 indicates that southern elephant seals spend the majority of the winter months in the ice foraging for food. The majority of CTD-SRDL

observations are found in the western part of the region. It is also important to note that some southern elephant seals dive in areas of open ocean and into the MIZ. One dive may be seen at the Antarctic coastline at 14°W.

a)

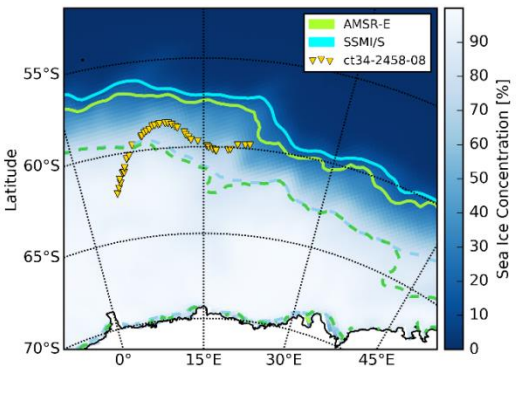

b)

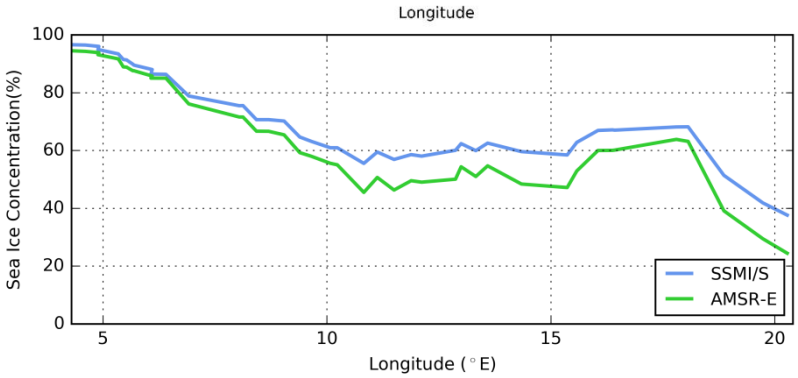

c)

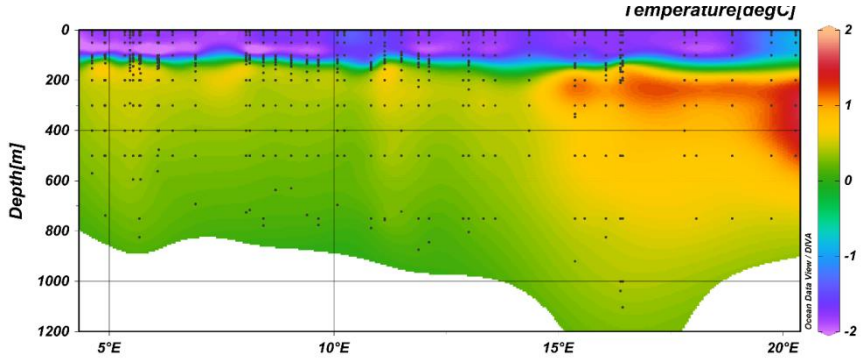

d)

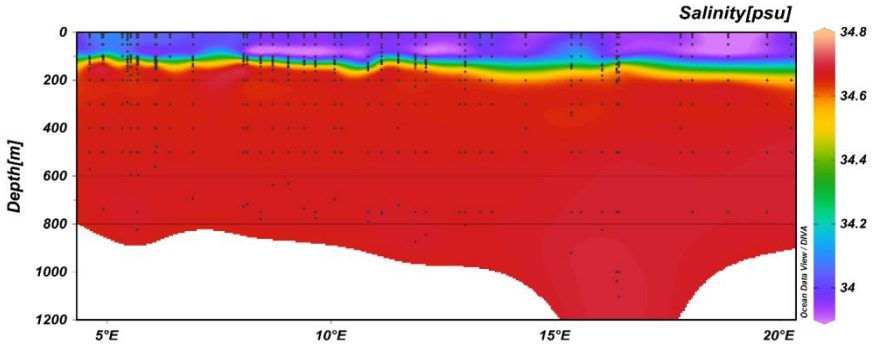

Figure 12: (a) Map of a trajectory of seal ct34-2458-08 (yellow) for the month of July 2008 based on location relative to the 15% SIC line. The map indicates the 15% (solid line) and 80% (broken line) SIC lines using the AMSR-E (green) and SSMI/S (blue) sensors. (b) Daily changes in SIC as the seal travels. (c) Cross section of temperature and (d) salinity to a depth of 900m which runs from 5°E to 20°E. The DIVA (Troupin et al., 2012) interpolation scheme is based on analysis of variance.

a)

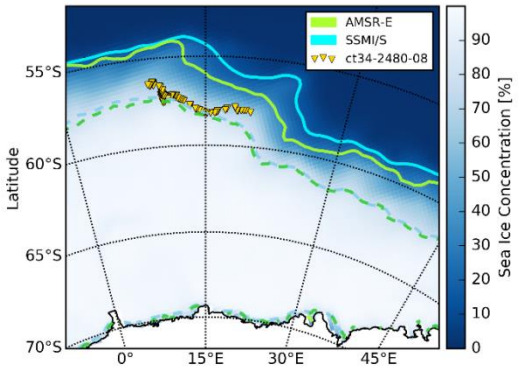

b)

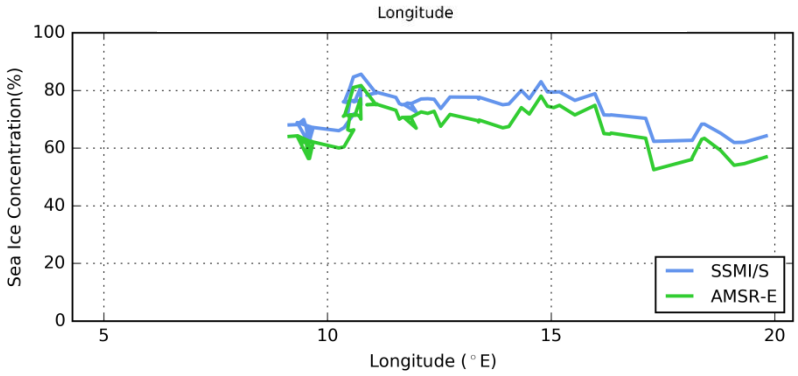

c)

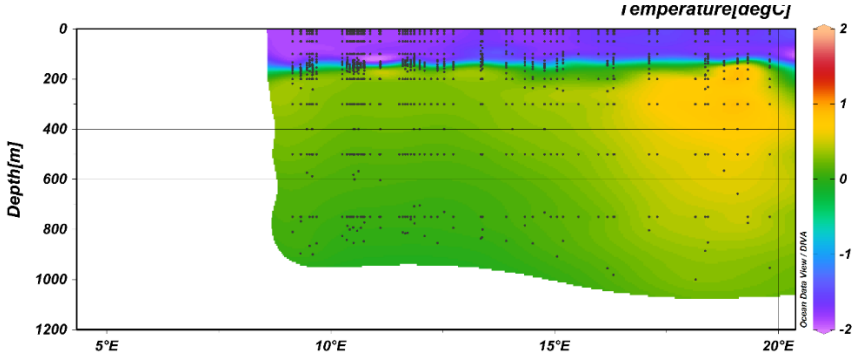

d)

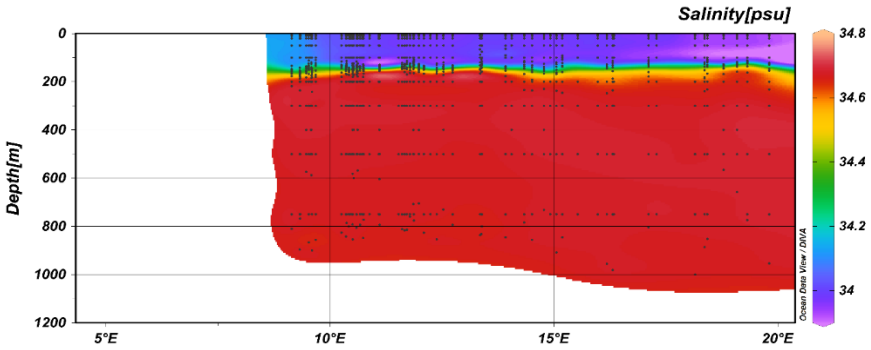

Figure 13: Map of the trajectory of seal ct34-2480-08 (yellow) for the month of August 2008 based on location relative to the 15% SIC line (a). The map indicates the 15% (solid line) and 80% (broken line) SIC lines using the AMSR-E (green) and SSMI/S (blue) sensors. Daily changes in SIC are seen as the seal travels (b). A cross section is also shown for temperature(c) and salinity (d) to a depth of 900 metres which runs from 5°E to 20°E. The DIVA (Troupin et al., 2012) interpolation scheme is based on analysis of variance.

Examples of cross sections within the MIZ are shown in Figs 12 and 13. These tracks occur at roughly the same latitude for two different animals during July and August.

In both July and August, the surface waters are cooler than the underlying waters at a temperature of -1 to -2°C. The thermocline and halocline shift from 150 metres in July to around 180 metres in August. This deepening occurs in both the western and eastern parts of the region. However, when looking at the east-west sections of each month, the western sections from 15°E appear to have deeper and cooler thermoclines and haloclines than the east. The positions of these tracks (Figs 12a and 13a) are also important as many profiles occur further south of the MIZ during the month of July.

The most visible feature in the cross section is the pool of relatively warm water in the east of the region below 180 m (Figs 12c and 13c). This pool has its core at 18°E and extends westward to 16°E. This warmer pool of water extends down to 900 m, is 2°C warmer than the subsurface waters above and it is more prominent in July than August. The water in July was not only warmer than August (Fig. 13c), but it also covers a larger area in the east of the region.

The warmer water masses in the east are associated with reduced SIC as seen in Figs 12b and 13b. This is more evident in Fig. 12b in the month of July. In July the profiles in the west are located further south than those in the east. This latitudinal change may also affect the SIC. It appears that a decrease in SIC relates to a deepening of the thermocline and halocline. Both months also indicate distinct changes in salinity (Fig. 13d). Fresher surface waters are seen in the east of the region than the west.

a)

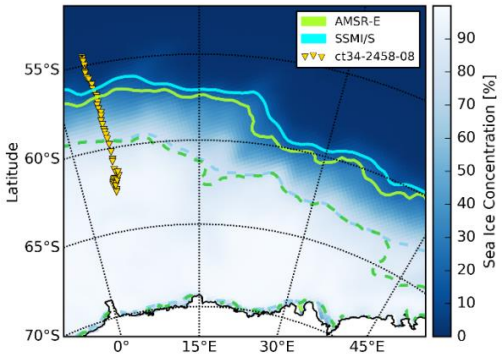

b)

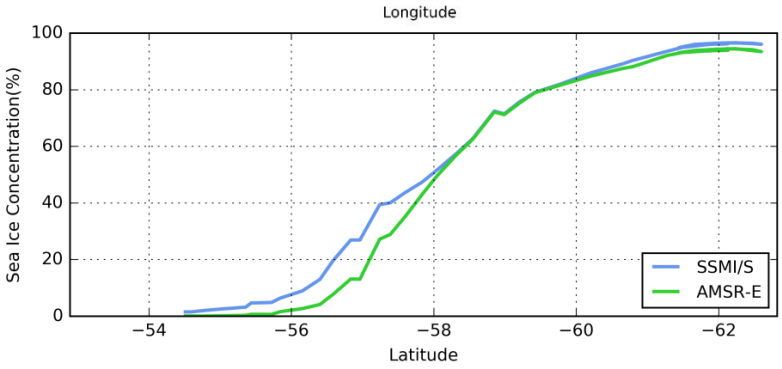

c)

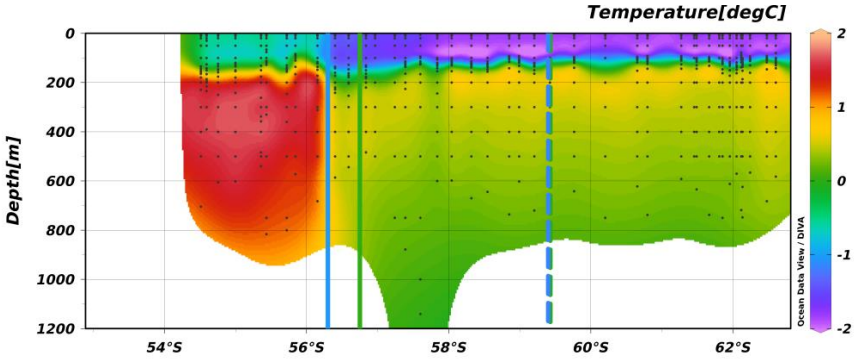

d)

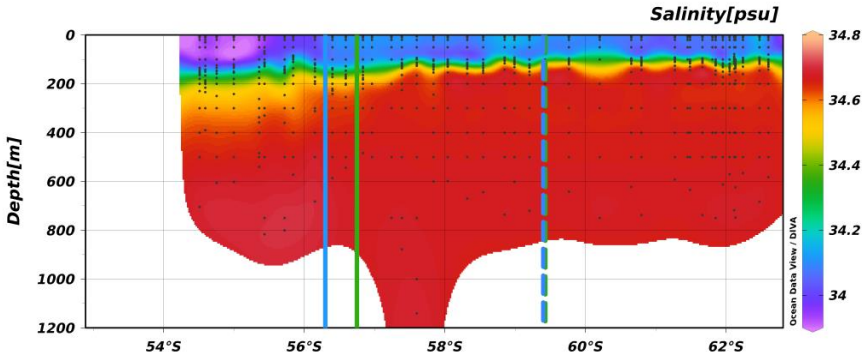

Figure 14: (a) Map of the trajectory of seal ct34-2458-08 (yellow) for the month of July 2008 based on location relative to the 15% SIC line. The map indicates the 15% (solid line) and 80% (broken line) SIC lines using the AMSR-E (green) and SSMI/S (blue) sensors. (b) Daily changes in SIC are seen as the seal travels. (c) Cross sections are also shown for temperature and (d) salinity to a depth of 900m which runs from 53.5°S to 62.3°S. The DIVA (Troupin et al., 2012) interpolation scheme is based on analysis of variance.

a)

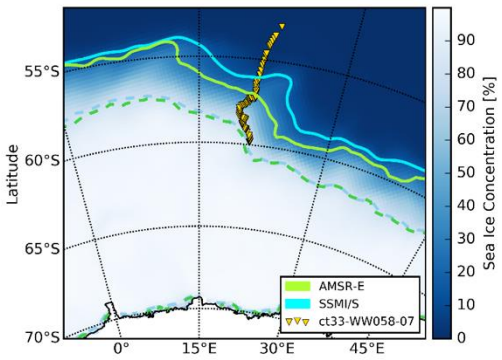

b)

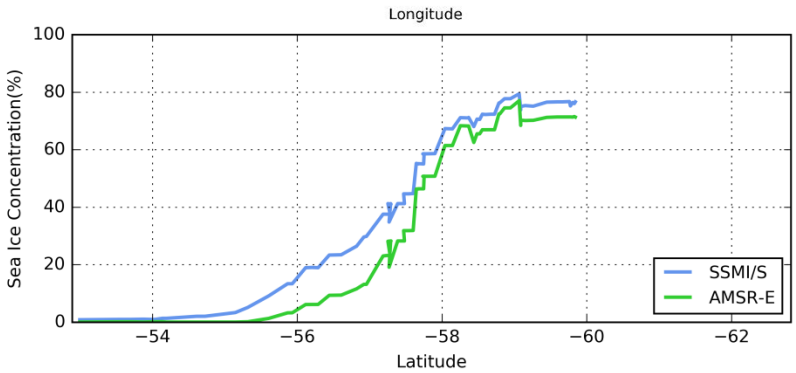

c)

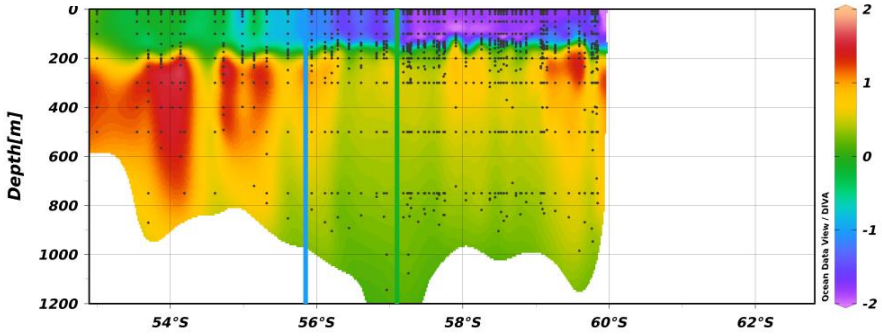

d)

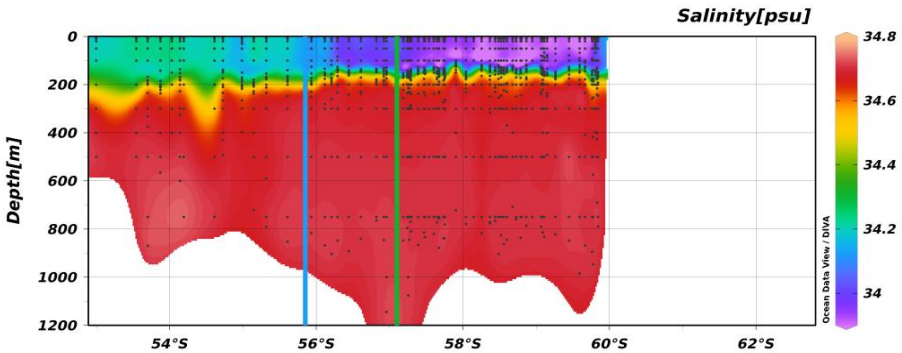

Figure 15: Map of the trajectory of seal ct34-WW058-07 (yellow) for the month of August 2007 based on location relative to the 15% SIC line (a). The map indicates the 15% (solid line) and 80% (broken line) SIC lines using the AMSR-E (green) and SSMI/S (blue) sensors. Daily changes in SIC are seen as the seal travels (b). A cross section is also shown for temperature(c) and salinity (d) to a depth of 900m which runs from 53.5°S to 62.3°S. The DIVA (Troupin et al., 2012) interpolation scheme based on variation analysis is used.

The same seal with ID ct34-2458-08 used in Fig.12 is used for Fig. 14. It travelled both through the MIZ and along the MIZ during July. Considering both pathways may further explain differences seen north to south or east to west. Figs 14a and 15a show meridional cross sections that traverse the MIZ from the open ocean in July and August, respectively. It is unfortunately not possible to find trajectories from the same region as in the previous case. This should to be taken into consideration as SIC is not consistent at the same latitude (see Fig. 8 compared to Fig. 11b). As indicated above in Figs 8 and 9, both months show that the SSMI/S data approximates the 15% SIC line further north than the AMSR-E data. The SSMI/S approximations are consistently further north than the AMSR-E approximations.

Open ocean waters (Figs 14c and 15c) have warmer subsurface waters in the north of each cross section in July and August. This relatively warm pool of water below the thermocline can be as much as 2°C warmer than the underlying water to the south of it. This warm pool of water is not apparent above the thermocline. Moreover, the surface water above this warm pool is warmer than the surface water in MIZ. The warm pool extends to 56.4°S in July but only reaches 55°S in August; it is also more prominent in July than August. The undulations along the thermocline and halocline in open waters further north (Figs 14 and 15) suggest turbulence and mixing.

The water above the thermocline appears to cool south of the 15% SIC line by 1 - 2°C. The month of July shows the MIZ water above the thermocline to become saltier than the surface salinity of the open waters (Fig. 14d). In contrast, the water above the thermocline in the MIZ becomes less salty than that further north in August (Fig. 15d). Apart from this surface difference, salinities do not show any distinct differences below the halocline during July and August. Note that the depth of the halocline and thermocline differ from month to month

Changes in surface salinity and temperature are clearly related to the edge of the MIZ (Figs 14 and 15). As SIC increases, surface temperatures decrease, and surface salinity increases during July (Fig. 14). The same changes in temperature occur in August but waters become less saline (Fig. 15).

3.4 The July water columns in the MIZ and in the open ocean

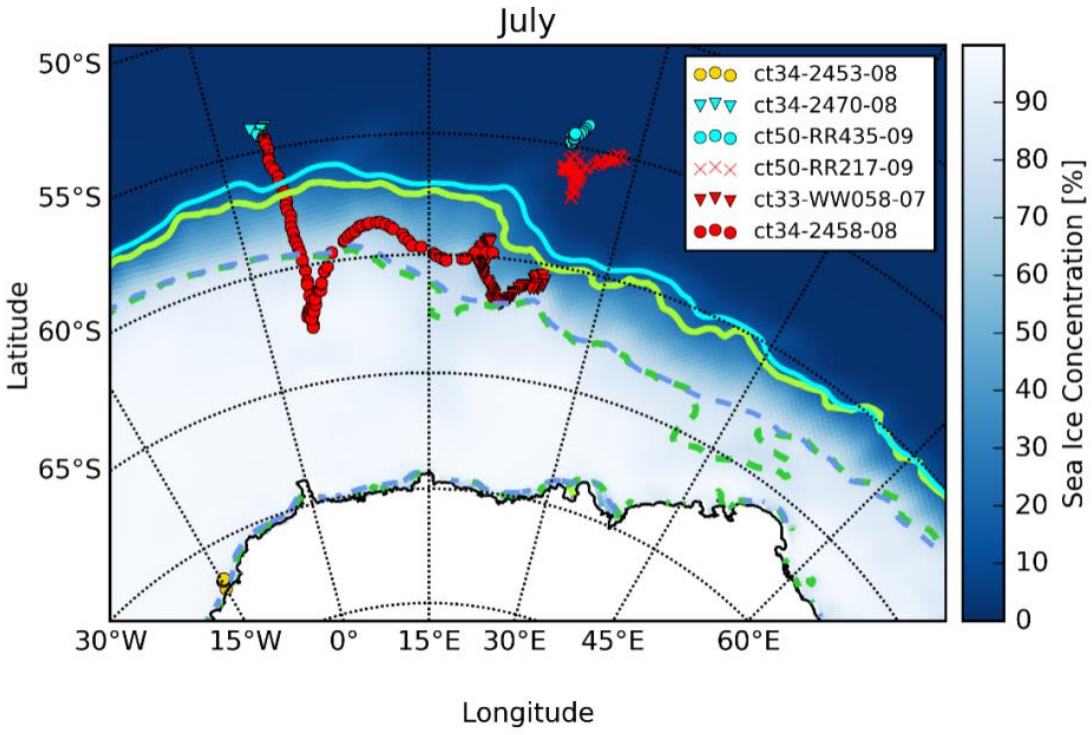

Figure 16: Map showing the distribution of selected CTD-SRDL observations for the month of July from 2005 to 2009. Profiles were selected based on their locations and seal IDs. The solid lines represent the 15% SIC line and the broken lines represent the 80% SIC line as calculated by using the AMSR-E (green) and SSMI/S (blue) satellite sensors. Locations consist of open ocean (blue profiles), 15-80% SIC (red profiles) and SIC higher than 80% (yellow profile). Note that one series of red profiles is purposefully located just north of the MIZ.

Open ocean CTD-SRDL observations with IDs ct34-2470-08 (blue triangles) and ct50-RR435-09 (blue circles) were taken from 55°S and northwards (Fig. 16) during 2008 and 2009, respectively. Three sets of profiles were taken in the MIZ, each representing different pathways within and around the MIZ. The MIZ seal with ID ct50-RR217-09 (red crosses) was selected just north of the MIZ to represent transitional physical features between the open ocean and the MIZ. This area is also an area of interest as ice sea ice occurs at the same latitude in the west of the region. Seal ct33-WW058-07 (red triangles) was selected as it lies consistently within the MIZ and seal ct34-2458-08 (red circles) shows a transition from an area of little to no sea ice into the MIZ. Seal ct34-2453-08 at the Antarctic coastline (orange

circles) shows an observation well south of the 80% SIC line of the MIZ and it is used as comparison with the Antarctic coastal region around 70° S.

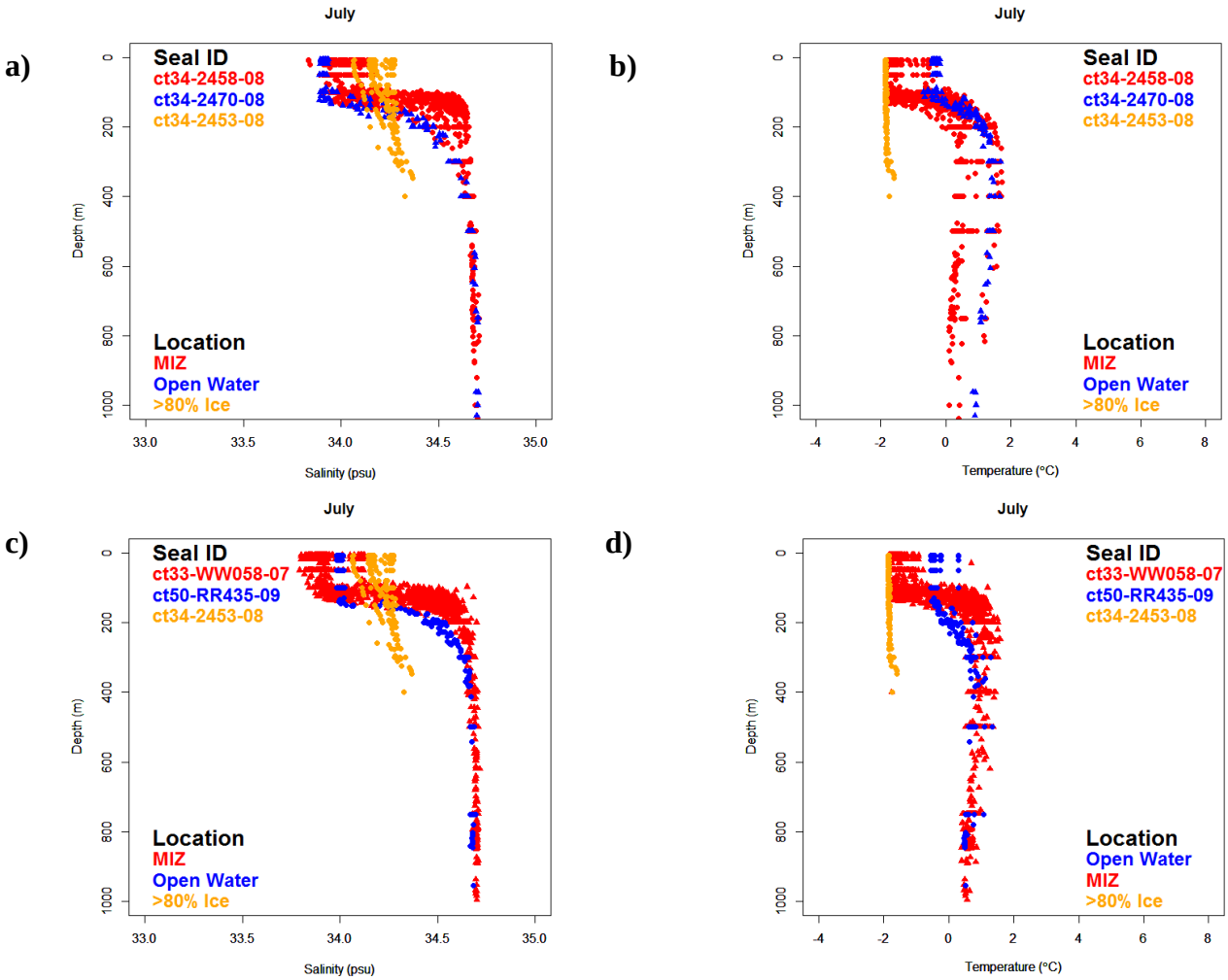

Figure 17: All profiles from five tagged southern elephant seals of salinity (a and c) and temperature (b and d) for the month of July 2005 to 2009. Profiles are shown from the MIZ seals with ID ct34-2458-08 (a and b) and ct33-WW058-07(c and d). The CTD-SRDL observations move from open ocean (blue) to the area of 15-80% SIC (red) to SIC which exceeds 80% (yellow).

Salinity values are generally higher in the surface layer of the MIZ relative to open ocean (Fig. 17a), although the MIZ profiles (red) show a large range in salinity at the halocline. Contrary to this, seal ct33-WW058-07 shows fresher water at the surface compared to open ocean (Fig. 17c). Note that the profiles of seal ct34-2458-08 (Fig 17a) are in the west of the region and seal ct-WW058-07 (Fig 17c) are in the east. There is little difference between the MIZ waters and the open ocean below 300m, suggesting that the influence of ice formation

processes can extend down to this depth. Profiles from ct34-2453-08 show saline water in the surface layer and the freshest water below the halocline.

Figs 17 b, d depict the coldest temperatures of -2 °C in the profile located south of the MIZ (yellow) where sea ice exceeds the concentration of 80%. The MIZ profiles (red) also show the largest ranges in temperature at the surface. The MIZ profiles also show generally colder temperatures than the open water (blue) profiles, with some variability below 300m depth (uniform salinities above).

a) **b)**

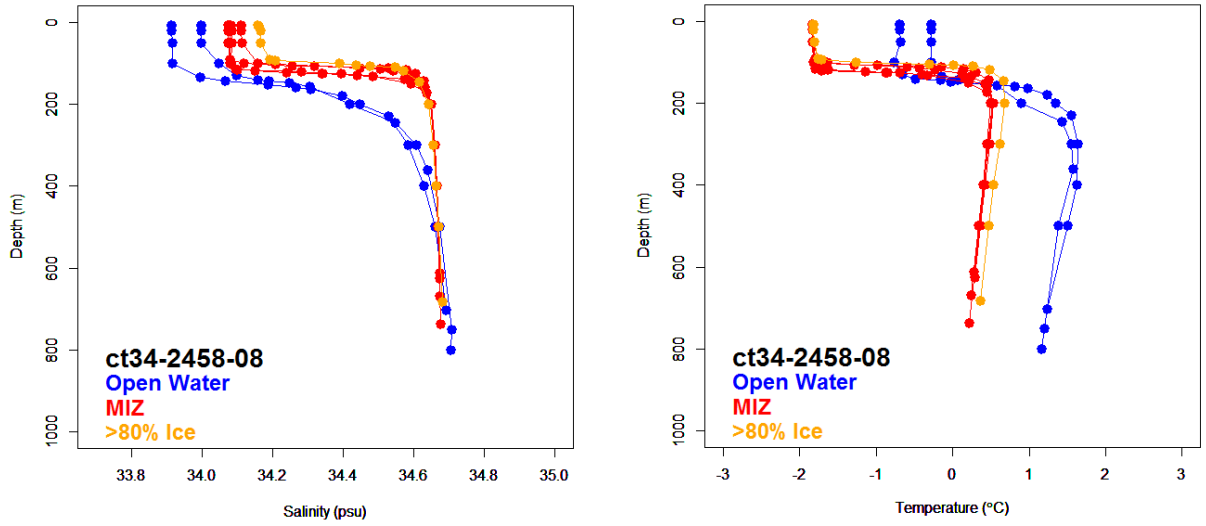

Figure 18: Individual profiles of one southern elephant seal (ID ct34-2458-08) for (a) salinity and (b) temperature during July 2008. The profiles move from open ocean (blue) to the MIZ (red) to SIC which exceeds 80% (yellow).

Data from the same MIZ seal of ID ct34-2458-08 used in Fig. 13 is analysed further in Fig. 18a to show the changes in the vertical profiles when crossing the MIZ. This figure clarifies that there is an increase in surface salinity and a shallower halocline moving from north to south of the MIZ during July. In the MIZ, profiles show sharper salinity gradients with depth. The halocline ranges from 180m in open water to 145m in areas where sea ice concentration is higher than 80%. At 400m depth, salinities in all profiles reach around 34.7 psu and remain relatively consistent down the water column.

The temperature features (Fig. 18b) are reversed. Above the thermocline, which ranges from 160 metres in the MIZ to 180 metres in open waters; temperatures are lower within the MIZ than in open waters. The change in the thermocline depth is not as much as that of the halocline depth (Fig 18a). It is also interesting to note that waters below the thermocline in the MIZ are 1 °C colder than profiles in the open ocean. This difference is shown to remain for the whole depth of the recorded dive (800 m). The difference in temperature below the thermocline is also apparent in the cross section (Fig. 14).

a) **b)**

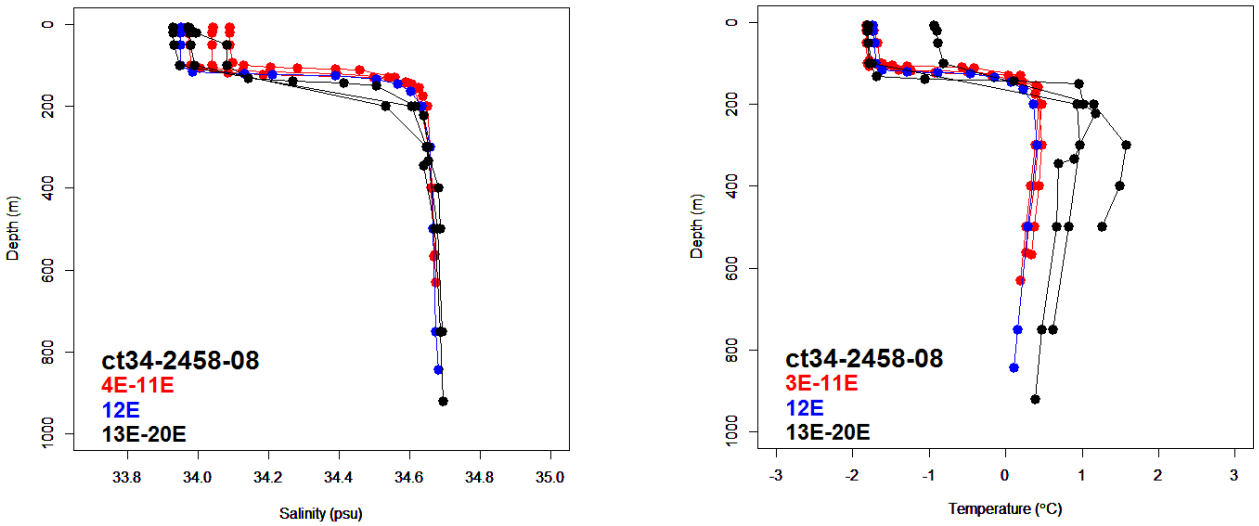

Figure 19: Individual profiles of one southern elephant seal with ID ct34-2458-08 for (a) salinity and (b) temperature for the month of July 2008. The profiles move from the west of the region (red) to the east (black). Profiles are 2° longitude apart. 12°E is considered to be the midpoint of the selected profiles.

Data from the seal (with ID ct34-2458-08) used in Figs 13 and 14 was also subjected to zonal trajectory analysis. The individual profiles show that surface salinities in the west of region are generally saltier than in the east (Fig. 19a). Slightly shallower haloclines are found in the west of the region. Below 200m, all profiles reach a salinity of about 34.7, which increases slightly with depth. The same cannot be said for temperature: below 200m, temperatures are warmer in the east of the selected trajectory than in the west (Fig. 19b). This is not as clear in surface temperatures where only one profile in the east has higher temperatures than the others.

3.5 The August water columns in the MIZ and in the open ocean

The same method was used in August as in July although the track locations differ from those of July.

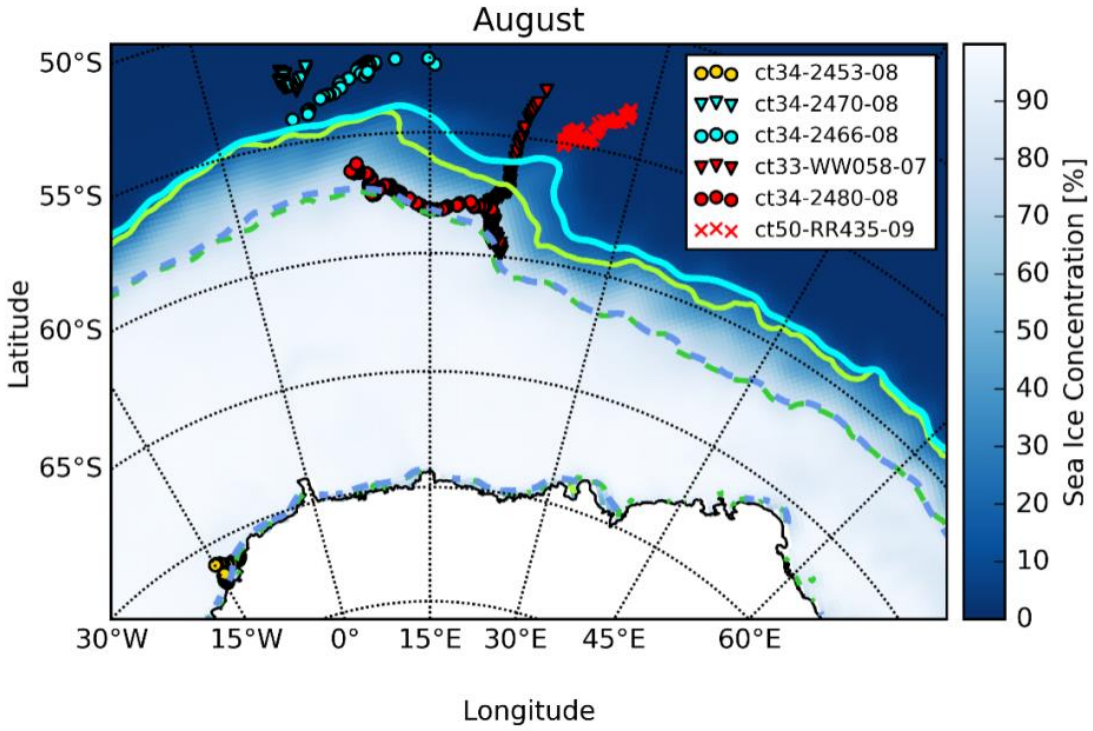

Figure 20: Map showing the distribution of selected CTD-SRDL observations for the month of August 2005 to 2009. Selected profiles were chosen based on their location and seal IDs. The solid lines represent the 15% SIC line and the broken lines represent the 80% SIC line as calculated by using the AMSR-E (green) and SSMI/S (blue) satellite sensors. Locations are open ocean (blue profiles), MIZ (red profiles) and SIC higher than 80% (yellow profile). Note that one series of red profiles is purposefully located just north of the MIZ.

Six trajectories for August are selected based on their location relative to the MIZ as well as southern elephant seal IDs (Fig. 20). Two trajectories are selected in sea ice-free waters well north of the MIZ. The trajectory of ct34-2480-08 is selected based on its position along the MIZ. Ct33-WW058-07 shows the transition from sea ice free water into the MIZ. A MIZ trajectory with ID ct50-RR435-09 is also selected just north of the MIZ to study water properties where SIC is less than 15%. The same seal (with ID ct34-2453-08) analysed close to Antarctica in July (Fig. 16) is also present close to Antarctica in August (Figs 20, 21).

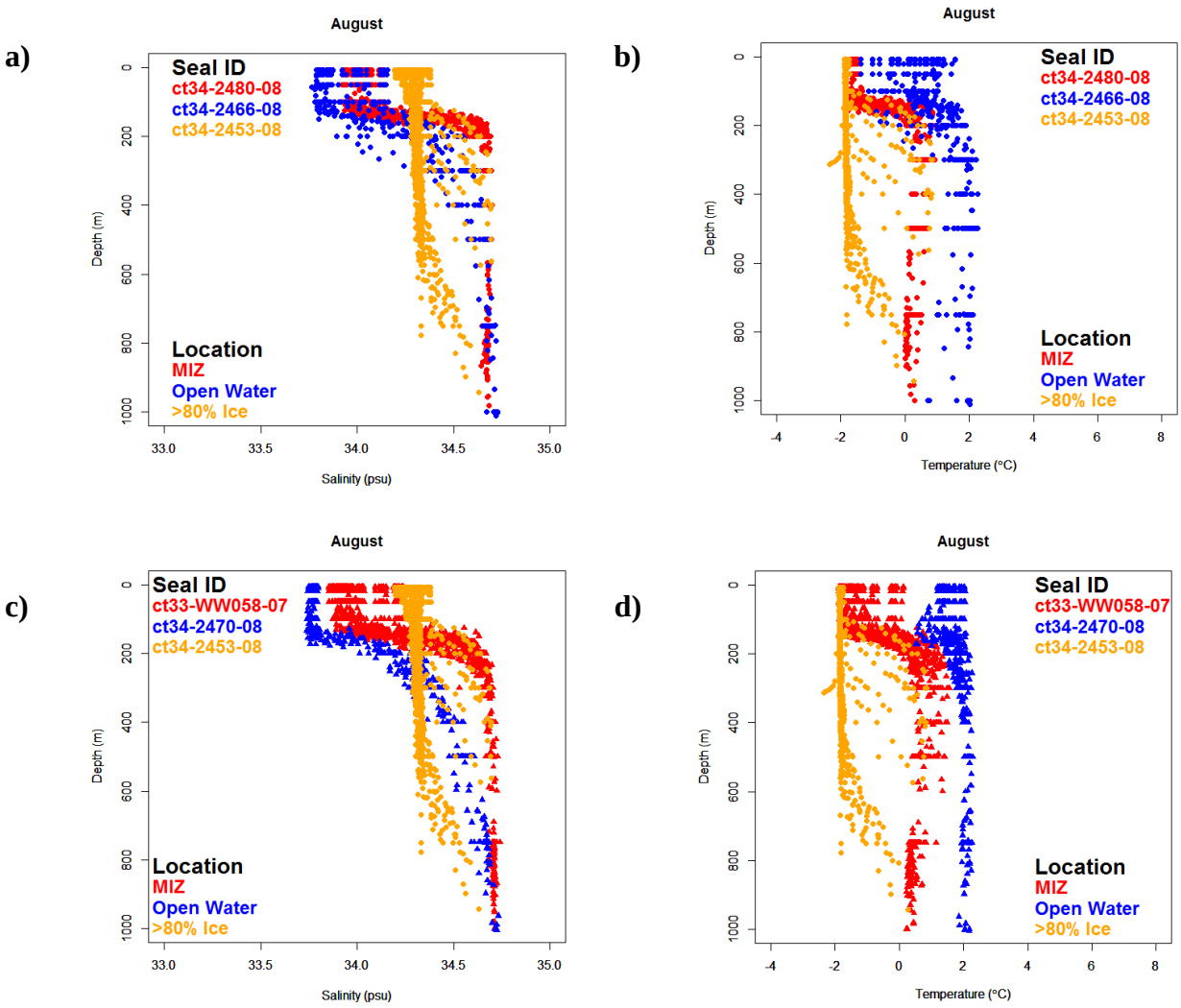

Figure 21: All profiles from five tagged southern elephant seals of (a, c) salinity and (b, d) temperature during August 2005 to 2009. The profiles of MIZ seals with ID ct34-2480-08 (a and b) and ct33-WW058-07(c and d) are presented. The CTD-SRDL observations move from open ocean (blue) to the MIZ (red) to SIC which exceeds 80% (yellow).

The largest changes in salinity between locations occur in the surface layer during August (Fig. 21). The halocline becomes shallower further south in the MIZ. There appear to be slight differences in salinity below the halocline which are not found in July profiles. However, general trends are similar in that as ice cover increases, salinities at the surface increase. With depth, the profiles with sea ice higher than 80% appear to be fresher than those of the open ocean and MIZ profiles. The MIZ profiles appear to be more saline than the open water profiles down to 800m depth (Fig. 21c)

Based on changes in the thermocline and halocline, the open ocean profiles show a deeper mixed layer (Fig. 21). This is shallower in the MIZ. Cooler temperatures are found in the MIZ compared to the open ocean and these differences persist with depth.

a) **b)**

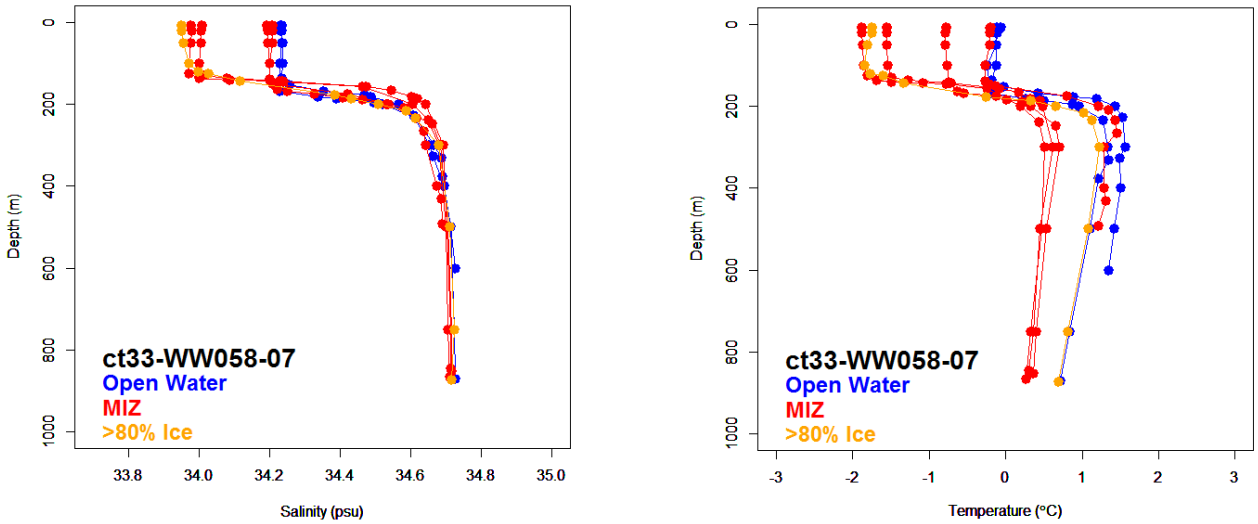

Figure 22: Individual profiles of southern elephant seal with ID ct33-WW058-07 for (a) salinity and (b) temperature for the month of August 2007. The profiles move from open ocean (blue) to the MIZ (red) and close to Antarctica (yellow).

The data of the seal in Figs 15 and 21 is analysed for changes in temperature and salinity with respect to latitude and SIC (Fig. 22). Fresher waters occur at the surface as SIC increases (Fig 22a). The opposite is true for the month of July (Fig. 18a). The top of the halocline appears to be slightly shallower as SIC increases. The halocline ranges from 175m to 200m which is deeper than that of July.

Surface temperature ranges from -1.94 to 0.13 °C (Fig. 22b). The MIZ shows the largest change in temperature at the surface. There is variability among MIZ profiles with depth. The MIZ also shows temperatures to be colder with depth than the profiles free of sea ice.

3.6 Water mass analyses

Behrendt et al. (2011) describe Winter Water (WW) formation with warm deep water present at depth. They also show that WW and warmer deep water (WDW) are present in the region of the present study. TS diagrams are presented here to investigate possible changes in the

water masses within the MIZ. The CTD-SRDL observations used in the cross sections (Figs 12-15) are also used in the water mass analysis. The pools of WDW described by Behrendt et al. (2011) are seen in the selected tracks.

July 2008 **August 2007(d) and 2008(b)**

a) **b)**

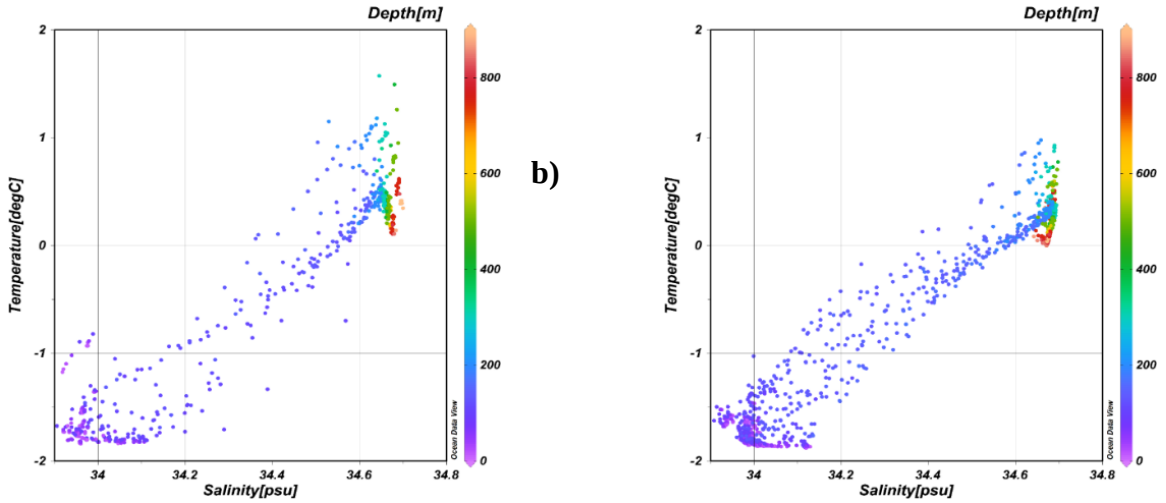

c) **d)**

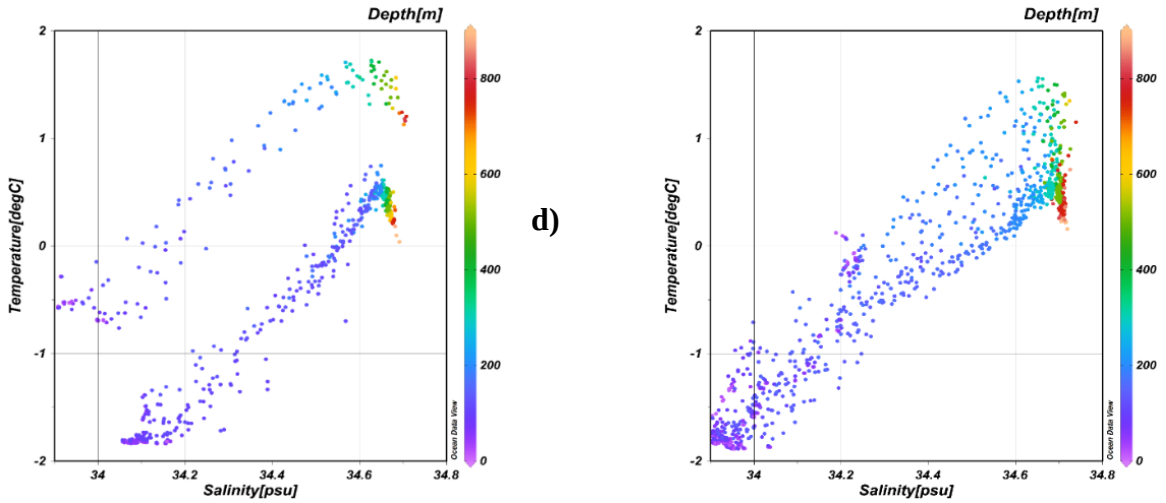

Figure 23: TS diagrams for July 2008 and August 2007 and 2008. (a) July profiles in the MIZ. (b) August Profiles in the MIZ, (c) July profiles from open water and into the MIZ (d) August profiles from open water and into the MIZ. Based on the data presented in Figs 12-15. Temperature was measured in degrees Celsius and salinity in practical salinity units.

The TS properties appear to show the same water mass for the month of July in all locations (Fig. 23). The water masses found in the open ocean do not differ from those found in the MIZ. Waters are shown to increase in temperature and salinity with depth down to about 400m. Temperatures and salinities decrease steadily below 400m. Fig. 23c shows a distinct change in temperature of about 1°C with latitude that is believed to be north of the polar front (Belkin et al. 1996).

August shows a similar pattern to July. However, the distinct temperature change (Fig 23d) is not as clear as in July. The temperature range in the August TS diagram from open ocean into the MIZ (Fig. 23d) is larger than the August TS diagram of profiles found within the MIZ (Fig. 23 b).

4. DISCUSSION AND CONCLUSION

This study investigated the possibility of relating the sea ice concentration products of AMSR-E and SSMI/S satellite sensors using the ASI algorithm to sub-surface hydrography observations by southern elephant seals. Here we defined the Marginal Ice Zone (MIZ) as the region between 15% and 80% sea ice concentration (SIC) and found that the majority of seal dives are found in this region during winter. By relating the MIZ to sub-surface hydrography, we characterised the hydrographic properties of the MIZ. Furthermore, analysis of both satellite and in situ observation data revealed causal relationships between SIC and subsurface seawater properties.

4.1 The relationship between SIC and hydrography

The results of this study confirm the variability of hydrographic properties within the MIZ. This variability in temperature and salinity is possibly due to a number of factors including sea ice coverage and other external oceanographic features such as air sea interactions and thermohaline circulation.

Overall, the results agree with what is known from the literature (Weeks and Ackley, 1986). During the formation of sea ice, as sea ice cover increases surface salinities tend to increase, and surface temperatures decrease (Fletcher, 2007; Ohshima et al., 2013). As in the present study, Ohshima et al. (2013) used instrumented seals and show that there is a relationship between the presence of sea ice and the temperature and salinity of the surrounding seawater. Ohshima et al. (2013) show how the formation of the cold, dense Antarctic Bottom Water is linked to sea ice formation. In addition to Ohshima et al. (2013), Boehme et al. 2008 also uses instrumented seals to monitor frontal movement around the ACC in the South Atlantic Sector. This further reinforces the use of animal-borne observations and how important temperature fronts are in the study region.

The sea ice extent during the months of July and August is approximately similar using either of the satellite sensors AMSR-E and SSMI/S (Fig. 7). Sea ice extends furthest northward in

the western part of the study region (Figs 7 and 8). This suggests that sea ice formation occurs at different rates within the region. Cooler surface waters may be related to increasing sea ice cover (Figs 12-15). The change in temperature becomes most obvious around the outer margin of the MIZ.

As one approaches the MIZ from the north, it is possible to find cooler surface waters as well as less undulation in the thermocline and halocline, indicating less turbulence and/or internal waves. This is a manifestation of the progressive increase of SIC through the MIZ, which dampens the upper ocean dynamics.

The sections traversing the MIZ occur in the west of the region in July and the east of the region in August (Figs 14 and 15). Although surface decreases in temperature are seen in both cross sections, it is less salty in the MIZ during August than July. Open ocean waters are also fresher in August compared to the MIZ in July. The opposite is true for the month of August in the eastern part of the region. No major differences in salinity are seen below the halocline between the two months or between the east and west of the region. The month of July shows an increase in surface salinity southwards, which is what is expected from ice formation and brine rejection (Weeks and Ackley, 1986). Consequently, as SIC increases southwards, surface temperatures decrease further. Although surface temperatures decrease southwards, surface salinities increase southwards within the MIZ in July but decrease in August.

Cold surface waters are one of the conditions for the formation of sea ice (Fletcher, 2007). Once sea ice forms, surface temperatures decrease further and this promotes the formation of more sea ice. This is shown in the sections that traverse the MIZ (Fig. 14 and 15):increasing SIC is related to cooler seawater temperatures as one moves further south in the MIZ.

The MIZ shows a wide range in surface layer temperatures and salinities (Figs 17, 18, 21 and 22). Moreover, defining boundaries of the MIZ by using a reference concentration such as the 15% SIC line from satellites remains a challenge due to a lack of consistent satellite sensor data. This may be due to the structure and colour of the sea ice and/or satellite sensor limitations. In situ observations such as the CTD-SRDL data define these boundaries well in the tracks analysed using temperature and salinity measurements (Figs 12-15).

The properties of temperature and salinity agree with what Fletcher (2007) and Orsi et al. (1995) found in ice covered regions. However, within the region, the present study shows

that sea ice cover is not the only factor responsible for differences in subsurface properties. The present results show that temperature and salinity in the west of the study region differ from those in the east, and this deserves further explanations.

4.2 Differences in water masses of the MIZ

The western part of the region in Fig. 18 shows typical features of temperature and salinity due to ice formation, as suggested in section 4.1. Changes in temperature and salinity due to ice formation were also found in previous studies such as Orsi et al. (1995) and Ohshima et al. (2013). The western cross sections also show that the waters below the surface layer are warmer than the surface water (Fig. 14) which again emphasizes the cooling effect sea ice formation may have in the winter months. The waters underneath the ice become stratified due to cooling and brine rejection. A large change in temperature in Fig. 14 also suggests a frontal boundary.

The underlying waters of areas well within the MIZ would not be greatly influenced by the direct effects of the wind and atmosphere due to increased sea ice cover. This may explain why the thermocline just north of the MIZ (Figs 14 and 15)id deeper and becomes shallower in areas of increasing sea ice.

The eastern part of the region shows different features to the west. Temperatures are warmer in the east (Fig. 15) both at the surface and with depth and the waters freshen with increasing sea ice cover. Although sea ice does not extend as far north as in the west (Figs 7, 8, 9 and 10); the sea ice would be expected to have the opposite effect.

Warmer waters are consistently found in the east during both July and August (Figs 12 and 13). The start of the MIZ as approximated by the AMSR-E sensor is further south than the 15% SIC line of SSMI/S; thus the MIZ may be better defined using the SSMI/S data product. Considering satellite limitations on detecting the 15% SIC line, it is difficult to determine which product detects the start of the MIZ better (Drucker et al., 2003). Both satellite products also show a slight decrease in SIC in the east of the region. This decrease in SIC could be related to the warmer waters found in the east of the region as shown by the CTD-SRDL observations in the present study (Fig. 12).

The SSMI/S position of the 15% SIC line is closer to the frontal boundary (Figs 14 and 15) than the AMSR-E line which is near an area of a rapid change in surface temperature. This may explain why the SSMI/S lines are systematically further north than the AMSR-E lines (Fig. 9). It is difficult to judge which seawater temperatures relate best to the 15% SIC line and the MIZ (Figs 14 and 15).

It is suggested that the origin of the warm water in the east of the region may be a spin offs from mesoscale eddies (Durgadoo et al., 2010; Ansorge et al., 2015). Eddies from the SWIR carry relatively warm water into the MIZ. Durgadoo et al. (2010), Ansorge et al. (2015) and Massie et al. (2016) also show how eddies move southwards to the MIZ in the east of the present study region. This region appears to be biologically productive as seals were found to be particularly active within and around it. Ansorge and Lutjeharms (2005) and Durgadoo et al. (2010) give subsurface values for the eddies as 34.1 psu in salinity and 2-4 °C in temperature. The TS diagrams from Ansorge et al. (2015) within the core of these eddies around 55°S also show temperatures to vary from 0 to 2 °C as well as salinities varying from 33.8 to 34.65 psu. They also show that these eddies decrease in temperature as they move southwards; this may explain why temperatures in Figs 12, 13, 19, 23 are not as high as 4 °C. Although the warm pool of underlying water is found in both July and August, temperatures are lower in August (Fig. 12 and 13). This may be due to the eddy losing temperature with increased sea ice cover during August (Fig. 7). It is interesting that this warm pool is consistent over two months.

Not only are the temperatures warmer in the east of the region, but the waters are also fresher (Figs 18 and 22). One reason may be that the relatively warm eddies propagate into the MIZ and contribute to melting of sea ice. Another reason may be that some physical mechanisms, (such as the eddies inducing some local processes of mixing and upwelling) contribute to freshening and limiting the formation of sea ice. Sea ice melt may also be promoted through such mixing.

Although Fig. 18 in the MIZ shows a consistent cooling in surface waters, the underlying waters show distinct differences. Moving southward in the MIZ, surface salinities increase, and temperatures decrease (Figs 17 and 21). Both temperature and salinity increase at the surface. This is not true for the eastern region affected by the above-mentioned eddies. The presence of a warmer body of water is shown in the TS diagrams (Fig. 23). Temperatures over 1 °C are seen in the TS diagrams including observations of the possible eddy (Fig. 23d).

This is different from the TS diagram just north of the MIZ which shows the clear temperature front (Fig. 23c). This also emphasises that the west of the study region shows different features to those of the east.

Behrendt et al. (2011) (Fig. 2) show the same trend of T/S properties with depth as seen in Fig. 23. Temperature and salinity ranges in Behrendt et al. (2011) are similar to those of the CTD-SRDL data in the present study. Orsi et al. (1995) suggest that changes in temperature may be frontal related. The Southern Front has a temperature difference of about 1 °C. The CTD-SRDL data of the present study shows the same temperature difference.

Apart from temperature changes due to frontal position, the water mass appears to be the same throughout the region. The properties of salinity and temperature indicate that the water mass may be Winter Water (WW) as described by Behrendt et al. (2011). One typical water mass is shown after visually comparing these TS diagrams (Fig. 23) to existing TS diagrams of the region in Fig. 2 (Orsi et al. 1995). The TS diagrams have the same temperature and salinity signatures. The TS diagrams in the present study show an increasing trend in both temperature and salinity and then decrease around 600m. The same may be trend may be seen in Orsi et al. (1995).

Sea ice is one of many factors that may influence the subsurface properties of seawater. Other aspects also need to be taken into consideration like atmospheric forcing, surrounding bodies of water as well as any other factors which may contribute to the formation or melting of sea ice (Belkin et al., 1996; Fletcher, 2007).

4.3 Conclusion and Future Work

This study suggests a methodological protocol for combining CTD-SRDL observations with remotely sensed sea ice concentration. If more CTD-SRDL observations are made, multiple profiles may be looked at qualitatively to take forward the idea of relating subsurface properties to the extent of the MIZ.

Temperature and salinity differ within the MIZ as shown in Section 4.2. Other oceanographic features pertaining to the water masses may complicate a direct relationship between

hydrographic properties and the presence or formation of sea ice. These features along with their duration and effects need to be identified in the region. It may be possible to more accurately describe the causal relationship between hydrography and sea ice by taking hydrographic features into account, i.

There are distinct changes in temperature and salinity upon entering the MIZ. Such changes need to be further analysed within the MIZ and over a longer time frame with the aid of more seal data or other autonomous vehicles, because the changes in temperature and salinity at the edge of the MIZ may then be used to better characterise the boundary of the MIZ.

Additional observations are also needed to improve the reliability of the findings such as the warm pool of water in the east of the region and its temporal evolution. The MIZ remains greatly influenced by the formation, melting and movement of sea ice in the months of July and August. The region may be divided into areas affected by the relatively warm pool of underlying water and an area affected by increasing sea ice cover in winter. Temporal changes should also be considered. Analysing daily or weekly data may allow tracking of eddies and ultimately, the warmer mass of water in the east of the region. One can then make reasonable inferences as to the effect of this warmer pool of water entering the region.

Apart from the relatively warm pool of underlying water in the east, properties with respect to depth in temperature and salinity in the region appear to be consistent with previous literature. The results in winter could also be related to what may be found in autumn and early spring when there are *in situ* observations. This would show whether or not there is a consistent pool of warm water in the east. In order to understand sea ice dynamics in the east, it is necessary to understand the effects the warm pool of water may have on its surroundings.

Southern elephant seals tend to forage around the MIZ and preferentially exploit particular areas (Biuw et al., 2007). As a result, CTD-SRDL observations accumulate in these foraging areas. These instruments are prone to instrumental drift that can cause inconsistencies in the data. It is therefore important that the time of tagging is considered. Thus scientists cannot rely solely on these observations for the austral winter. Thus additional observation methods are required. Since there are few winter observations, using a combination of instruments such as gliders and floats would improve not only the area covered but also the resolution of data.

Numerical ocean models for the area may also help resolve features in conjunction with the findings of in situ observations. Other oceanographic features may also be accounted for by using models. Modelling features can contribute to conclusively define relationships between sea ice and hydrographic properties within the MIZ.

The spatial definition of the MIZ edge can be improved by increasing the number or type of satellite sensors. Recent satellite products such as that of the AMSR-2 sensor, which is a continuation of AMSR-E, can also be considered as ways of increasing SIC observations with time. Finer resolution may also be considered other than the 25 km used in this study. Algorithms other than ASI could also be used.

This study suggests that future work can be done to improve the quality and quantity of satellite and direct observations both spatially and temporally. Apart from subsurface hydrographic properties and sea ice contributions in the MIZ, the region is also influenced by winds and wave action. This may be considered by using reanalysis data which provides evidence of air-sea interaction. Monitoring and analysing these aspects at smaller time scales may give some insight into changes in the MIZ. Thus, considering all these factors will reinforce the potential of relating sea ice cover to hydrographic properties in the MIZ and how they affect one another.

5. REFERENCES

Adkins, J.F., McIntyre, K.& Schrag, D.P. 2002. The salinity, temperature, and δ18O of the glacial deep ocean. *Science.* 298(5599):1769-1773.

Andreas, E.L., Tucker, W.B. & Ackley, S.F. 1984. Atmospheric boundary-layer modification, drag coefficient, and surface heat flux in the Antarctic marginal ice zone. *Journal of Geophysical Research: Oceans.* 89(C1):649-661.

Ansorge, I.J., Jackson, J.M., Reid, K., Durgadoo, J.V., Swart, S. & Eberenz, S. 2015. Evidence of a southward eddy corridor in the south-west Indian Ocean. *Deep Sea Research Part II: Topical Studies in Oceanography.* 119:69-76.

Ansorge I.J. & Lutjeharms, J.R.E. 2002. The hydrography and dynamics of the ocean environment of the Prince Edward Islands (Southern Ocean). *Journal of Marine Systems.* 37:107-127.

Ansorge I.J. & Lutjeharms, J.R.E. 2003. Eddies originating at the South West Indian Ridge. *Journal of Marine Systems.* 39:1-18.

Ansorge, I.J. & Lutjeharms, J.R.E. 2005. Direct observations of eddy turbulence at a ridge in the Southern Ocean. *Geophysical Research Letters*. 32. DOI:10.1029/2005GL022588.

Aoki, S., Kitade, Y., Shimada, K., Ohshima, K.I., Tamura, T., Bajish, C.C., Moteki, M. & Rintoul, S.R. 2013. Widespread freshening in the Seasonal Ice Zone near 140° E off the Adélie Land Coast, Antarctica, from 1994 to 2012. *Journal of Geophysical Research: Ocean.* 118(11):6046-6063.

ASI Algorithm AMSR-E sea ice concentration were obtained for [PERIOD] from the Integrated Climate Date Center (ICDC, icdc.cen.uni-hamburg.de/), University of Hamburg, Hamburg, Germany

Behrendt, A., Fahrbach, E., Hoppema, M., Rohardt, G., Boebel, O., Klatt, O., Wisotzki, A. & Witte, H. 2011. Variations of Winter Water properties and sea ice along the Greenwich meridian on decadal time scales. *Deep Sea Research Part II: Topical Studies in Oceanography.* 58(25):2524-2532.

Belkin, I.M. & Gordon, A.L. 1996. Southern Ocean fronts from the Greenwich Meridian to Tasmania. *Journal of Geophysical Research: Ocean.* 101(C2):3675-3696.

Biuw, M., Boehme, L., Guinet, C., Hindell, M., Costa, D., Charrassin, J.B., Roquet, F., Bailleul, F., Meredith, M., Thorpe, S. & Tremblay, Y. 2007. Variations in behavior and condition of a Southern Ocean top predator in relation to in situ oceanographic conditions. *Proceedings of the National Academy of Sciences.* 104(34):13705-13710.

Biuw, M., Nøst, O.A., Stien, A., Zhou, Q., Lydersen, C. & Kovacs, K.M. 2010. Effects of hydrographic variability on the spatial, seasonal and diel diving patterns of southern elephant seals in the eastern Weddell Sea. *PLoS One*. 5(11):13816.

Bjørgo, E., Johannessen, O.M. & Miles, M.W. 1997. Analysis of merged SMMR-SSMI time series of Arctic and Antarctic sea ice parameters 1978–1995. *Geophysical Research Letters.* 24(4):413-416.

Boehme, L., Meredith, M. P., Thorpe, S. E., Biuw, M. & Fedak, M. 2008. Antarctic Circumpolar Current frontal system in the South Atlantic: Monitoring using merged Argo and animal-borne sensor data. *Journal of Geophysical Research: Oceans.* 113(C09012).

Boehme, L., Lovell, P., Biuw, M., Roquet, F., Nicholson, J., Thorpe, S.E., Meredith, M.P. & Fedak, M. 2009. Technical note: Animal-borne CTD-satellite relay data loggers for real-time oceanographic data collection. *Ocean Science.* 5:685–695.

Boyd, P.W. & Law, C.S. 2001. The Southern Ocean iron release experiment (SOIREE)—introduction and summary. *Deep Sea Research Part II: Topical Studies in Oceanography.* 48(11):2425-2438.

Brierley, A.S., Fernandes, P.G., Brandon, M.A., Armstrong, F., Millard, N.W., McPhail, S.D., Stevenson, P., Pebody, M., Perrett, J., Squires, M. & Bone, D.G. 2002. Antarctic krill under sea ice: elevated abundance in a narrow band just south of ice edge. *Science.* 295(5561):1890-1892.

Carmack, E.C. 2007. The alpha/beta ocean distinction: A perspective on freshwater fluxes, convection, nutrients and productivity in high-latitude seas. *Deep Sea Research Part II: Topical Studies in Oceanography.* 54(23):2578-2598.

Carrick, R., Csordas, S.E. & Ingham, S.E. 1962. Studies on the Southern elephant seal, Miroungaleonina (L.). IV. Breeding and development. *Wildlife Research*. 7(2):161-197.

Charrassin, J.B., Hindell, M., Rintoul, S.R., Roquet, F., Sokolov, S., Biuw, M., Costa, D., Boehme, L., Lovell, P., Coleman, R. & Timmermann, R. 2008. Southern Ocean frontal structure and sea-ice formation rates revealed by elephant seals. *Proceedings of the National Academy of Sciences*. 11(33):634-11639.

Charrassin, J.B., Roquet, F., Park, Y.H., Bailleul, F., Guinet, C., Meredith, M., Nicholls, K., Thorpe, S., Tremblay, Y., Costa, D. & Göbel, M. 2010. New insights into Southern Ocean physical and biological processes revealed by instrumented elephant seals. *Proceedings of OceanObs 09: Sustained Ocean Observations and Information for Society (Vol. 2)*, Venice, Italy, 21-25 September 2009, Hall, J., Harrison DE & Stammer, D., Eds., ESA Publication WPP-306.

Clarke, D.B. & Ackley, S.F. 1984. Sea ice structure and biological activity in the Antarctic marginal ice zone. *Journal of Geophysical Research: Oceans*. 89(C2):2087-2095.

Comiso, J.C. and Nishio, F. 2008. Trends in the sea ice cover using enhanced and compatible AMSR-E, SSM/I, and SMMR data. *Journal of Geophysical Research: Oceans*, 113(C2).

Constantin, A. & Johnson, R.S. 2016. An exact, steady, purely azimuthal flow as a model for the Antarctic Circumpolar Current. *Journal of Physical Oceanography*. 46(12):3585-3594.

Durgadoo, J.V., Ansorge, I.J. & Lutjeharms, J.R. 2010. Oceanographic observations of eddies impacting the Prince Edward Islands, South Africa. *Antarctic Science*. *22*(3):211-219.

Durgadoo, J.V., Ansorge, I.J., Lutjeharms, J.R., De Cuevas, B.A. & Coward, A.C. 2011. Decay of eddies at the South-West Indian Ridge. *South African Journal of Science*. 107(11-12):1-10.

Espedal, H.A., Johannessen, O.M. & Knulst, J. 1996. Satellite detection of natural films on the ocean surface. *Geophysical research letters.* 23(22):3151-3154.

Fedak, M. 2004. Marine animals as platforms for oceanographic sampling: a" win/win" situation for biology and operational oceanography. *Memoirs of National Institute of Polar Research. Special issue*. 58:133-147.

Fedak, M. A. 2013. The impact of animal platforms on polar ocean observation. *Deep Sea Research, Part II*. 88:7–13.

Fletcher, N.H. 2009. The chemical physics of ice. *The Chemical Physics of Ice, by NH Fletcher*. Cambridge, UK: Cambridge University Press.

Foster, T.D. & Carmack, E.C. 1976. Temperature and salinity structure in the Weddell Sea. *Journal of Physical Oceanography*. 6(1):36-44.

Freeland, H.J., Roemmich, D., Garzoli, S.L., Le Traon, P.Y., Ravichandran, M., Riser, S., Thierry, V., Wijffels, S., et al. 2010. Argo-a decade of progress. In OceanObs' 09: Sustained Ocean Observations and Information for Society (Vol. 2), Venice, Italy, 21-25 September 2009.

Gille, S. T. 2002. Warming of the Southern Ocean since the 1950s. *Science*. 295(5558):1275-1277.

Gloersen, P. & Campbell, W.J. 1991. Recent variations in Arctic and Antarctic sea-ice covers. *Nature*. 352(6330):33.

Gloersen, P., Campbell, W.J., Cavalieri, D.J., Comiso, J.C., Parkinson, C.L. & Jay Zwally, H. 1993. Satellite passive microwave observations and analysis of Arctic and Antarctic sea ice, 1978-1987. *Annals of Glaciology*. 17(1):149-154.

Gould, J., Roemmich, D., Wijffels, S., Freeland, H., Ignaszewsky, M., Jianping, X., Pouliquen, S., Desaubies, Y. et al. 2004. Argo profiling floats bring new era of in situ ocean observations. *Eos*. 85(19):179-184.

Hall, A. & Visbeck, M. 2002. Synchronous variability in the Southern Hemisphere atmosphere, sea ice, and ocean resulting from the annular mode. *Journal of Climate*. 15(21):3043-3057.

Jacobs, S. 2006. Observations of change in the Southern Ocean. *Philosophical Transactions of the Royal Society of London A: Mathematical, Physical and Engineering Sciences*. 364(1844):1657-1681.

Kaleschke, L., F. Girard-Ardhuin, G. Spreen, A. Beitsch& Kern, S. ASI Algorithm SSMI-SSMIS sea ice concentration data, originally computed at and provided by IFREMER, Brest, France, were obtained as 5-day median-filtered and gap-filled product for [PERIOD] from the Integrated Climate Date Center (ICDC, icdc.cen.unihamburg.de/), University of Hamburg, Hamburg, Germany.

Kaleschke, L., Lüpkes, C., Vihma, T., Haarpaintner, J., Bochert, A., Hartmann, J. & Heygster, G. 2001. SSM/I sea ice remote sensing for mesoscale ocean-atmosphere interaction analysis. *Canadian Journal of Remote Sensing*. 27(5):526-537.

Kikuchi, T., Inoue, J. & Langevin, D. 2007. Argo-type profiling float observations under the Arctic multiyear ice. *Deep Sea Research Part I: Oceanographic Research Papers.* 54(9):1675-1686.

Martinson, D.G. 1990. Evolution of the Southern Ocean winter mixed layer and sea ice: open ocean deepwater formation and ventilation. *Journal of Geophysical Research: Oceans*. 95(C7):11641-11654.

Massie, P. P., McIntyre, T., Ryan, P. G., Bester, M. N., Bornemann, H., and Ansorge, I. J. 2016. The role of eddies in the diving behaviour of female Southern elephant seals. *Polar Biology*, 39(2):297-307.

McIntyre, T., Ansorge, I.J., Bornemann, H., Plötz, J., Tosh, C.A. & Bester, M.N. 2011. Elephant seal dive behaviour is influenced by ocean temperature: implications for climate change impacts on an ocean predator. *Marine Ecology Progress Series*. 441:257-272.

Meredith, M.P. & Hogg, A.M. 2006. Circumpolar response of Southern Ocean eddy activity to a change in the Southern Annular Mode. *Geophysical Research Letters*. 33(16).

Mitchell, B.G., Brody, E.A., Holm-Hansen, O., McClain, C. & Bishop, J. 1991. Light limitation of phytoplankton biomass and macronutrient utilization in the Southern Ocean. *Limnology and Oceanography*. 36(8):1662-1677.

Ohshima, K.I., Fukamachi, Y., Williams, G.D., Nihashi, S., Roquet, F., Kitade, Y., Tamura, T., Hirano, D. et al. 2013. Antarctic Bottom Water production by intense sea-ice formation in the Cape Darnley polynya. *Nature Geoscience*. 6(3):235-240.

Orsi, A.H., Whitworth, T. & Nowlin, W.D. 1995. On the meridional extent and fronts of the Antarctic Circumpolar Current. *Deep Sea Research Part I: Oceanographic Research Papers*. 42(5):641-673.

Park, Y.H., Charriaud, E. & Fieux, M. 1998. Thermohaline structure of the Antarctic surface water/winter water in the Indian sector of the Southern Ocean. *Journal of Marine Systems*. 17(1):5-23.

Park, Y.H., Charriaud, E., Craneguy, P. & Kartavtseff, A. 2001. Fronts, transport, and Weddell Gyre at 30 E between Africa and Antarctica. *Journal of Geophysical Research: Oceans*. 106(C2):2857-2879.

Ren, M., Chen, J., Shao, K., Yu, M. & Fang, J. 2016. Quantitative prediction process and evaluation method for seafloor polymetallic sulfide resources. *Geoscience Frontiers*. 7(2):245-252.

Reynolds, R. W., Rayner, N. A., Smith, T. M., Stokes, D. C., & Wang, W. 2002. An improved in situ and satellite SST analysis for climate. *Journal of climate*. 15(13):1609-1625.

Riser, S.C., Freeland, H.J., Roemmich, D., Wijffels, S., Troisi, A., Belbéoch, M., Gilbert, D., Xu, J., Pouliquen, S., Thresher, A. & Le Traon, P.Y. 2016. Fifteen years of ocean observations with the global Argo array. *Nature Climate Change*. 6(2):145-153.

Roemmich, D., Riser, S., Davis, R. & Desaubies, Y. 2004. Autonomous profiling floats: Workhorse for broad-scale ocean observations. *Marine Technology Society Journal*. 38(2):21-29.

Roquet, F., Williams, G., Hindell, M.A., Harcourt, R., McMahon, C., Guinet, C., Charrassin, J.B., Reverdin, G. et al. 2014. A Southern Indian Ocean database of hydrographic profiles obtained with instrumented elephant seals. *Scientific data*. 1:140028.

Russell, J.L., Dixon, K.W., Gnanadesikan, A, Stouffer, R.J. & Toggweiler, J.R. 2006. The Southern Hemisphere Westerlies in a Warming World: Propping Open the Door to the Deep Ocean. *Journal of Climate*. 19.

Serreze, M.C., Maslanik, J.A., Scambos, T.A., Fetterer, F., Stroeve, J., Knowles, K., Fowler, C., Drobot, S., Barry, R.G. and Haran, T.M. 2003. A record minimum arctic sea ice extent and area in 2002. *Geophysical Research Letters*. 30(3).

Shimada, K., Kamoshida, T., Itoh, M., Nishino, S., Carmack, E., McLaughlin, F., Zimmermann, S. & Proshutinsky, A. 2006. Pacific Ocean inflow: Influence on catastrophic reduction of sea ice cover in the Arctic Ocean. *Geophysical Research Letters*, 33(8).

Sloyan, B.M., &Rintoul, S.R. 2001. The Southern Ocean limb of the global deep overturning circulation. *Journal of Physical Oceanography*. 31(1):143-173.

Smith, S.L., Smith, W.O., Codispoti, L.A. & Wilson, D.L. 1985. Biological observations in the marginal ice zone of the East Greenland Sea. *Journal of marine research*. 43(3):693-717.

Spreen, G., Kaleschke, L. & Heygster, G. 2008. Sea ice remote sensing using AMSR-E 89-GHz channels. *Journal of Geophysical Research: Oceans*. 113(C2).

Stroeve, J.C. & Campbell, G.G. 2016. Mapping and assessing variability in the Antarctic marginal ice zone, pack ice and coastal polynyas in two sea ice algorithms with implications on breeding success of snow petrels. *The Cryosphere*. 10(4):1823.

Strong, C., Foster, D., Cherkaev, E., Eisenman, I. & Golden, K. 2017. On the definition of marginal ice zone width. *Journal of Atmosphere Oceanic Technology*. 34: 1565–1584. doi:10.1175/JTECH-D-16-0171.1.

Toudal, L. 1999. Ice extent in the Greenland Sea 1978–1995. *Deep Sea Research Part II: Topical Studies in Oceanography*. 46(6):1237-1254.

Toyota, T., Ukita, J., Ohshima, K.I., Wakatsuchi, M. & Muramoto, K.I. 1999. A measurement of sea ice albedo over the southwestern Okhotsk Sea. *Journal of the Meteorological Society of Japan. Ser. II*. 77(1):117-133.

Troupin, C., Barth, A., Sirjacobs, D., Ouberdous, M., Brankart, J.M., Brasseur, P, Rixen, M, Alvera Azcarate, A. et al. 2012. Generation of analysis and consistent error fields using the Data Interpolating Variational Analysis (Diva). *Ocean Modelling*. 52-53:90-101.

Turk, F.J. & Miller, S.D. 2005. Toward improved characterization of remotely sensed precipitation regimes with MODIS/AMSR-E blended data techniques. *IEEE Transactions on Geoscience and Remote Sensing*. 43(5):1059-1069.

Wadhams, P., Squire, V.A., Goodman, D.J., Cowan, A.M. & Moore, S.C. 1988. The attenuation rates of ocean waves in the marginal ice zone. *Journal of Geophysical Research: Oceans*. 93(C6):6799-6818.

Weeks, W.F. & Ackley, S.F. 1986. The growth, structure, and properties of sea ice. In *The geophysics of sea ice.* N. Untersteiner. New York: Springer. 9-164.

Weissling, B., Ackley, S., Wagner, P. & Xie, H. 2009. EISCAM—Digital image acquisition and processing for sea ice parameters from ships. *Cold Regions Science and Technology*. 57(1):49-60.

Worby, A.P., Geiger, C.A., Paget, M.J., Van Woert, M.L., Ackley, S.F. & DeLiberty, T.L. 2008. Thickness distribution of Antarctic sea ice. *Journal of Geophysical Research: Oceans*. 113(C5).

Zhang, Q. & Skjetne, R. 2015. Image processing for identification of sea-ice floes and the floe size distributions. *IEEE Transactions on Geoscience and Remote Sensing*. 53(5):2913-2924.

Appendices

Appendix A

Monthly SIC Maps and the Distribution of CTD-SRDL Observations for the Years 2005-2009.

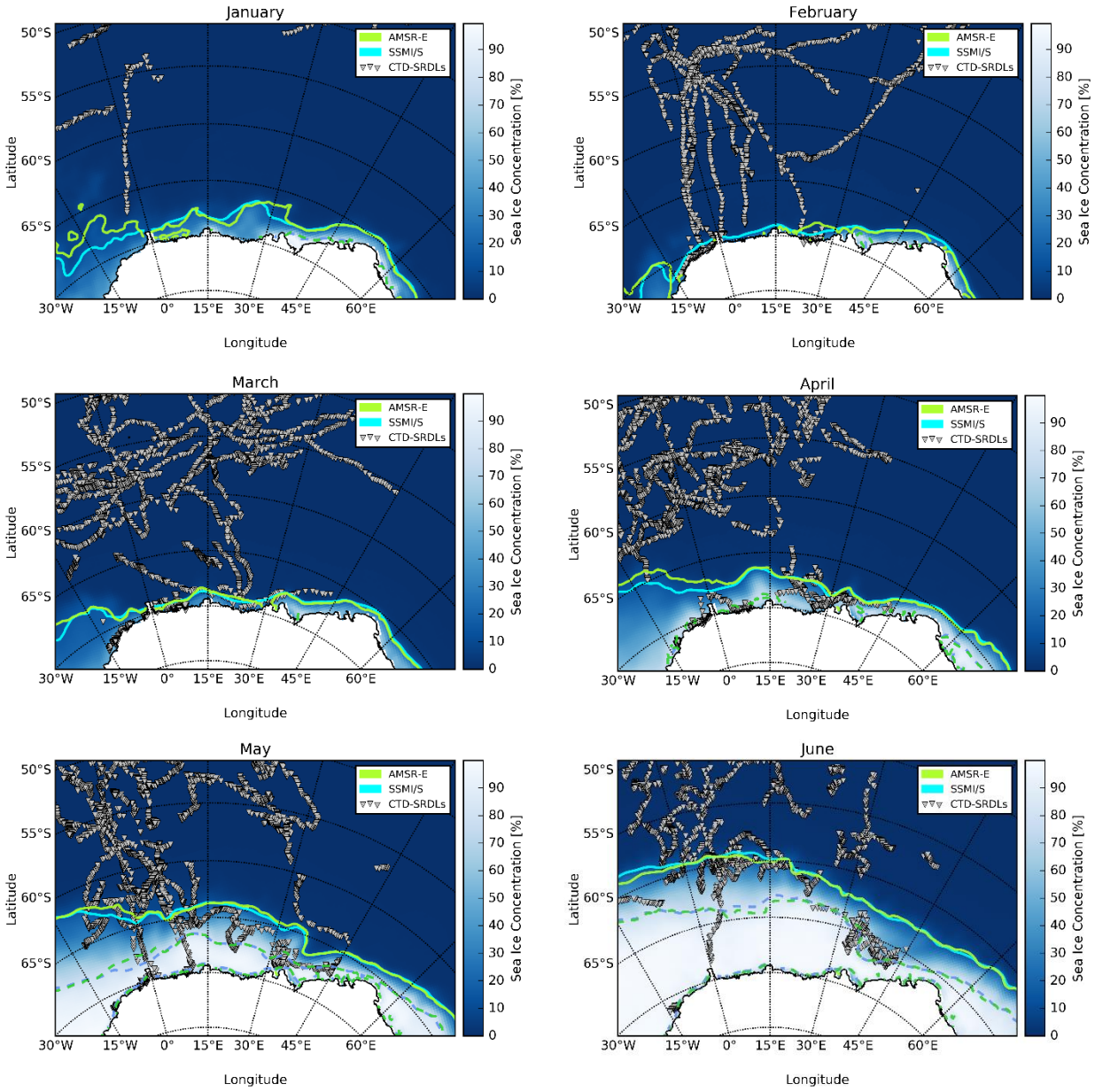

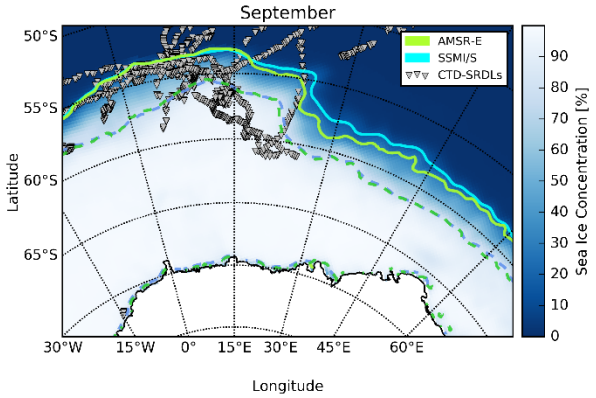
September
AMSR-E
SSMI/S
CTD-SRDLs
50°S
55°S
60°S
65°S
Latitude
30°W
15°W
0°
15°E
30°E
45°E
60°E
Longitude
Sea Ice Concentration [%]
0
10
20
30
40
50
60
70
80
90

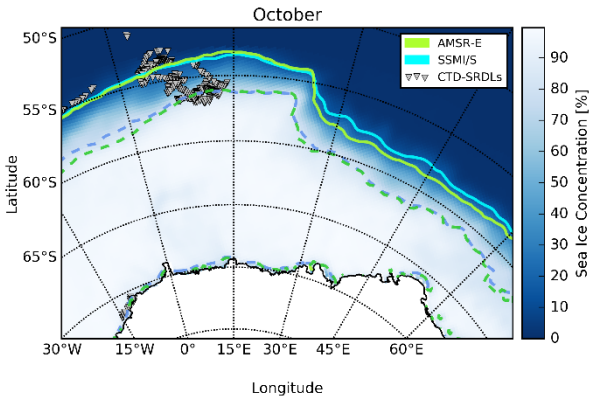
October
AMSR-E
SSMI/S
CTD-SRDLs
50°S
55°S
60°S
65°S
Latitude
30°W
15°W
0°
15°E
30°E
45°E
60°E
Longitude
Sea Ice Concentration [%]
0
10
20
30
40
50
60
70
80
90

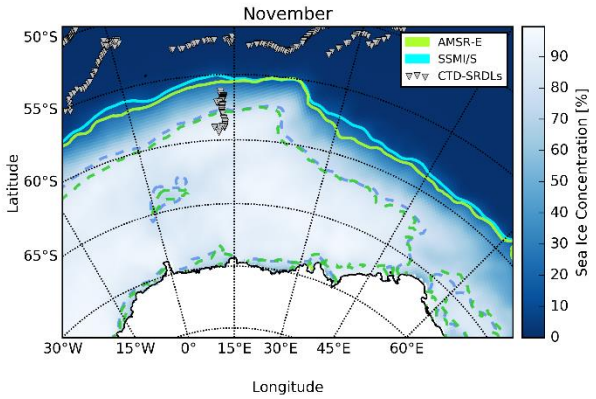
November
AMSR-E
SSMI/S
CTD-SRDLs
50°S
55°S
60°S
65°S
Latitude
30°W
15°W
0°
15°E
30°E
45°E
60°E
Longitude
Sea Ice Concentration [%]
0
10
20
30
40
50
60
70
80
90

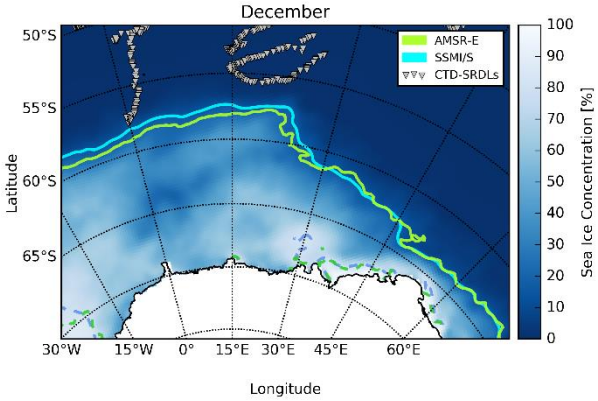
December
AMSR-E
SSMI/S
CTD-SRDLs
50°S
55°S
60°S
65°S
Latitude
30°W
15°W
0°
15°E
30°E
45°E
60°E
Longitude
Sea Ice Concentration [%]
0
10
20
30
40
50
60
70
80
90
100